AutoGaitA – Automated Gait Analysis in Python

M. Hosseini[1], I. Klein[2], T. D. Kuzu[2], C. Semmler[2], V. Wunderle[2], V. Mardare[3], A. Galvao[2], M. Haustein[4], A. Büschges[4], C. Grefkes[2,5], T. Korotkova[3], G. R. Fink[1, 2], P. H. Weiss[1, 2], G. Gatto[2]*, S. Daun[1, 4]*

1 Institute of Neuroscience and Medicine (INM-3), Forschungszentrum Jülich, Germany

2 Department of Neurology, University Hospital of Cologne, Germany

3 Institute of Systems Physiology, University Hospital of Cologne, Germany

4 Institute of Zoology, University of Cologne, Germany

5 Department of Neurology, University Hospital Frankfurt

*co-corresponding authors: s.daun@fz-juelich.de; graziana.gatto@uk-kolen.de;

Author Note

[This work was funded by the Deutsche Forschungsgemeinschaft (DFG, German Research Foundation) - Project-ID 431549029-INF, 431549029-Z02, 431549029-Z03, SFB 1451]

Abstract

Animals change their location in space by means of walking, running, swimming, or flying, a series of rhythmic motor behaviours that together are defined as locomotion. Individual types of locomotion require a unique coordinated pattern of muscle contractions that can be inferred by the location of joints across the body. Implementations of recent advancements in machine learning (ML), such as DeepLabCut and Simi Shape, have automated the tracking of body posture, even in markerless subjects. Despite ML algorithms alleviating the tracking effort, making sense of the tracked points still requires substantial amounts of manual labour and lacks standardisation across research labs. To this end, we developed *AutoGaitA* (Automated Gait Analysis), an open-source Python toolbox designed to automate the analysis of locomotion by normalising the step cycle, extracting meaningful features from the tracked coordinates (e.g. angles, velocity, acceleration) and allowing intra- and inter-animal comparisons. Here, we employed *AutoGaitA* in a series of proof of principles experiments to show age-dependent changes in locomotion in flies, mice and humans, age-dependent changes in adaptation mechanisms in mice, and to compare the key features of walking across species. *AutoGaitA*'s adaptability to any kind of motor behaviour and any species of interest makes it a valuable tool for the motor community to standardise the analysis of rhythmic behaviours across genotypes, disease states and species.

Introduction

Locomotion refers to the animal's ability to change their location in space via the engagement of rhythmic motor behaviours, including, for example, walking, running, swimming, or flying. Each of these rhythmic motor behaviours can be deconstructed in two phases (e.g. stance and swing during walking, forward and backward stroke in swimming) and requires unique patterns of coordinated muscle activity within and across body limbs (Grillner et al. 2020). Coordinated muscle contractions define the position of joints and their relative positions in space as animals locomote. Physiological and pathological perturbations affect the ability of animals to coordinate their body during the execution of locomotion, significantly affecting intra- and interlimb coordination (Grillner et al. 2020). Many labs have identified pathologies in humans and animal models (Boyer et al., 2017; Dougherty, 2023; Stolze et al., 2000; Zanardi et al. 2021) causing locomotor dysfunctions, yet the customised analysis algorithms, the selected parameters chosen, and the different ways to normalise step-cycle phases render it difficult to compare these results and correlate, for example, walk impairments in rodent models and human patients having the same mutation or pathology. Thus, establishing a tool for the automated analysis of locomotion will enable the standardised comparison across experimental groups, species, and laboratories, allowing the identification of conserved principles of motor control and adaptation.

Recent advancements in machine learning (ML) have automated body posture tracking, even in markerless living beings, with two examples being DeepLabCut (DLC, Mathis et al., 2018) and Simi Shape (henceforth just called Simi, Winiarski, 2003). These ML models can be trained to recognise body parts (joints or other points of interest, e.g. ears and nose) in video recordings of behaving animals and humans and output the 2D or 3D coordinates over time. Although ML algorithms have alleviated the tracking effort, making sense of the tracked coordinates still requires

substantial amounts of manual labour and lacks standardisation across research labs. Custom-made scripts are often tailored to species- and locomotor-specific paradigms, such as ladder or treadmill walking (Aljovic et al., 2022), and built to compare experimental groups based on predefined sets of parameters. Developing these scripts is cumbersome and often limits the power of the analysis by restricting it to few in-built kinematic features that are hard to re-program. Furthermore, scripts are often customised to camera brands, tracking algorithms, or terminology preferred by individual labs. Therefore, we developed *AutoGaitA* (Automated Gait Analysis), an open-source Python toolbox designed to automate the analysis of locomotion, normalising the step cycle, extracting meaningful and customisable features from the tracked coordinates (e.g. angles, velocity, acceleration), and allowing intra- and inter-animal comparison.

We defined multiple features that render *AutoGaitA* a valuable tool for the motor community: a) simplification of the workflow of motor scientists via automating a wide range of tasks; b) provision of a flexible tool that can analyse many motor behaviours and be independent of the species studied; c) extraction of features that are meaningful for scientists on a case-to-case basis and high-sensitive detection of changes in motor coordination; d) definition of common readouts for intra- and cross-species comparisons.

We designed a simple workflow to convert joint/keypoint coordinates tracked with ML-based algorithms (DLC and Simi Shape) into standardised comparable graphs and datasets, simplifying the study and interpretation of locomotion. We show three examples to demonstrate *AutoGaitA*'s utility in assessing locomotor changes in response to two perturbations (age and beam width) and across three species (fly, mouse and human).

In summary, we developed a novel toolbox that, by standardising and automating various analysis steps and simplifying the workflow of (loco-)motor studies, provides a useful resource to

define common readouts and better compare motor dysfunctions induced by physiological and pathological perturbations across species and labs.

Results

Developing a novel toolbox for locomotion analysis

We developed a Python-based toolbox, *AutoGaitA* (software doi: Hosseini, 2024), to simplify, fasten and streamline the analysis of locomotor features from the coordinates generated with ML-based body posture tracking algorithms. Notably, despite being developed for mouse and human locomotor analysis, our toolbox can be effectively employed to analyse any rhythmic behaviour in any species of interest, including invertebrates. To facilitate the user experience, our toolbox consists of three distinct and independent graphical user interfaces (GUIs): *AutoGaitA_DLC* and *AutoGaitA_Simi* to analyse body coordinates tracked with DLC and Simi, respectively, and *AutoGaitA_Group* to compare up to 6 groups of interest, like mouse genotypes or patient cohorts. Nevertheless, experienced users can access *AutoGaitA's* full capabilities via the command line.

AutoGaitA analysis of 2D locomotor kinematics: from tracked coordinates to standardised graphs

Workflow

The workflow of *AutoGaitA_DLC* requires three consecutive steps (preparatory work, main configuration, and run analysis), plus an optional step for advanced settings (**Figure 1A**). In the first step, prior to the analysis, users need to standardise the name of the coordinate files tracked with DLC to a default naming convention (see *AutoGaitA_DLC's Detailed User Workflows* in the Appendix) and generate an Excel table with timestamp annotations of the rhythmic cycle (*Annotation Table*). In case of walking, the Annotation Table contains timestamps detailing the

beginning of swing, end of swing and end of stance (see also template of *Step Cycle Annotation Table*). The correct preparation of files (**Figure 1A**) is crucial, and in-depth guidelines, templates and example datasets can be found in the *Detailed User Workflows* section below and in our online documentation repository (link)

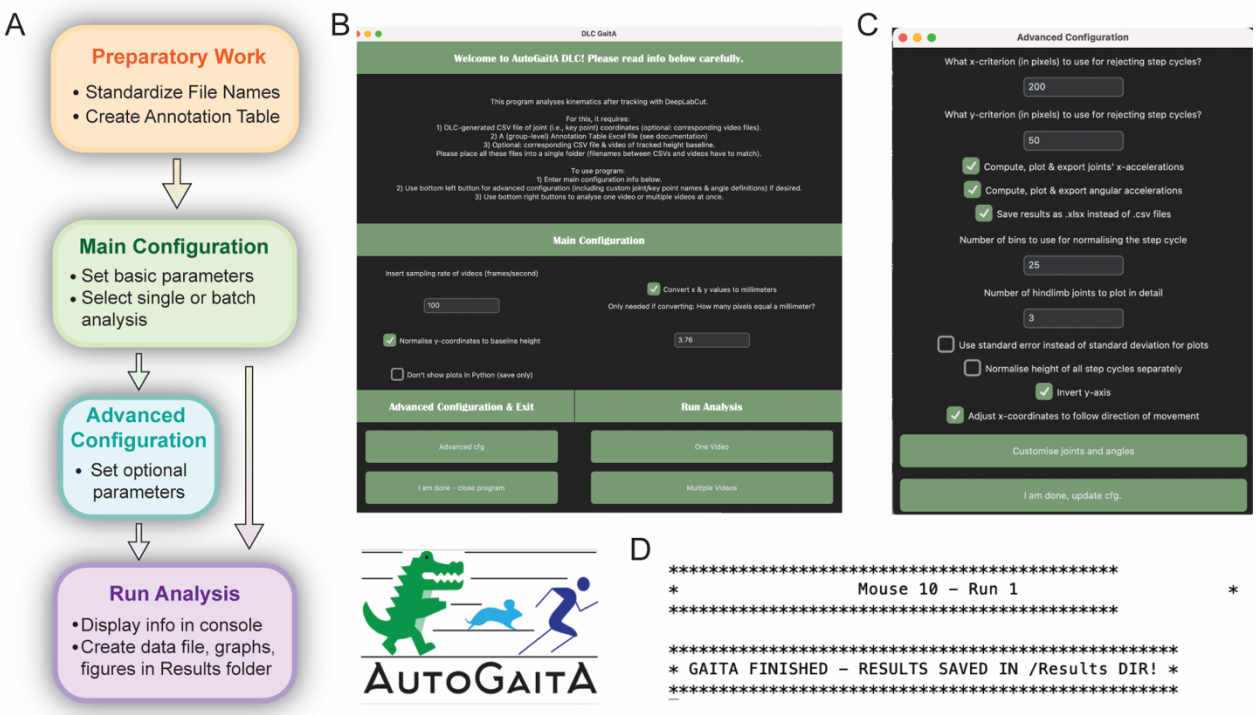

Figure 1. AutoGaitA_DLC workflow. A) *Schematic representing the steps to analyse data with AutoGaitA_DLC.* ***B,C)*** *Snapshots of the Main (**B**) and Advanced (**C**) Configuration windows.* ***D)*** *Snapshot of the Console window during the analysis.*

After the initial step is completed, users need to set the basic parameters in the Main Interface window, e.g. frame rate at which videos were acquired and pixel-to-mm conversion factor (**Figure 1B**). After selecting single or batch analysis, *AutoGaitA_DLC* will prompt them to set the directory where the DLC-coordinate files and the *Annotation Table* are located and the unique identifiers composing the file names (see *Detailed User Workflows*). At this point, users can run the analysis or configure additional optional parameters (**Figure 1C**), like selecting specific joints, calculating

acceleration, and plotting standard error rather than standard deviation (see also *Detailed User Workflows* in the Appendix). Once all parameters are set, the analysis can be run.

As the analysis is running, data information, warnings, and errors are displayed in Python's command window (**Figure 1D**). For each analysed video, a separate subfolder is generated in the *Results* folder in which respective data files and figures are stored (see also *Detailed User Workflows* in the Appendix).

Toolbox Description

We developed *AutoGaitA_DLC* to extract, calculate, normalise and average meaningful features from DLC-tracked 2D coordinates (Mathis et al. 2018) of individuals performing rhythmic motor behaviours and thus simplifying the statistical comparisons across experimental groups, species, and behavioural paradigms. *AutoGaitA_DLC* a) quality-checks the tracked coordinates, b) corrects for inconsistencies in the direction of walking or in the terrain surface, c) derives angles from the joint coordinates, d) calculates velocities and accelerations of joints and angles, e) normalises kinematic features within individual steps, f) compiles excel files with the results, and g) generates standardised graphic visualisations of the data (see also *Detailed User Workflows*).

The algorithm reads the *Annotation Table* and runs an automatic accuracy check of the tracking by verifying that changes in coordinates between neighbouring time points are within reasonable spatial limits. For example, if the mouse ankle moves 18 cm within 10 msec, it is counted as a tracking failure and the corresponding step cycle is automatically excluded from further analyses. The threshold of these spatial limits is pre-set to a default value, but users are advised to revise it in the *Advanced Configuration* window based, for example, on their video resolution and the distance of the animal from the camera.

The toolbox additionally offers the possibility to correct for inconsistencies in the direction or surface animals walk on, e.g. an uneven floor or a beam. In the same experimental setup, animals might walk from left to right or vice versa. To make data independent of the direction of motion, we implemented an option to adjust the horizontal coordinates (henceforth called x-coordinates) and simulate that all animals walk towards the same point. The vertical coordinates (henceforth called height or y-coordinates in mice) are normalised either to a baseline height obtained by tracking the floor or the beam with DLC to provide reference values or to the overall lowest y-coordinate in each dataset. In the latter case, it is recommended to normalise each step for the lowest y-coordinate value if the floor is uneven or cameras are distorted (see also *Detailed User Workflows*).

Following these built-in data quality controls, *AutoGaitA_DLC* retrieves the data for each joint, or, more generally, each keypoint (or landmark), and computes angles. Hindlimb joints (hindpaw, ankle, knee, hip, and iliac crest) and angles (ankle, knee, and hip) are set as default but can be fully customised in the *Advanced Configuration* window. Thus, any angle can be derived as long as the coordinates of three points defining it are provided. Next, *AutoGaitA_DLC* computes horizontal joint and angular velocities and, if desired, accelerations.

At this point, step cycles are normalised to be of equal length by setting each step length to 100% and dividing it into the default but customisable value of 25 bins. That is, if step cycles are longer than 25 timepoints, they are shortened by averaging the data values of neighbouring time points to fit in 25 bins. For example, if a step cycle contains 50 timepoints, we average the first and second timepoints, the third and fourth, and so on so that the original 50 timepoints fit in 25 bins. If step cycles contain less than 25 timepoints, data values are repeated to fit in 25 bins. For

example, a step cycle with 23 timepoints is fit in 25 bins by repeating the first and second data points.

AutoGaitA_DLC allows the analysis of a single dataset (one video of an individual trial) or the batch analysis of all datasets stored in a specific folder (see detailed instructions for both approaches in the *Detailed User Workflows* and our online documentation). For each analysed video or trial, results are saved in individual subfolders within the *Results* folder created in the same directory where the datasets are stored. Results include the analysed data compiled in Excel files (raw and normalised values of individual step cycles, averages, and standard deviation across all steps for each input video), standard Figures saved as *png* and *svg* (vector image format) files, the input (DLC) files analysed, and a text file describing potential issues about the data, the configuration, or the analysis. The vector image format allows users to customise graphs and best adapt them to their desired style and colour palette (see also *Showcase examples*). Finally, *AutoGaitA_DLC* generates a variety of figures, including stick diagrams for the hindlimb and forelimb, joint coordinates and angles over time, and trial averages of all the kinematic features. These first-level results can be further analysed using *AutoGaitA_Group* to assess differences across, e.g. experimental conditions, species, ages, or disease states.

Acquisition of 3D kinematics with Simi and 2D locomotor analysis with AutoGaitA

AutoGaitA_Simi has been developed to extract meaningful 2D kinematic features from Simi-tracked 3D coordinates (Winiarski, 2003) of animals or human participants performing rhythmic motor tasks. Although *AutoGaitA_Simi* is very similar to *AutoGaitA_DLC*, and the workflow presented in **Figure 1** also largely applies to the analysis of Simi data, there are some key differences. First, *AutoGaitA_Simi* was developed to decode 3D joint coordinates of subjects walking back and forth, with each trial including periods of continuous walking in between turning

points, and step cycle data include coordinates for both legs. Thus, we implemented an in-built "auto-rotation" feature that reverses the direction of walking so that all steps are consistent in their horizontal coordinates (back to forth). This feature is analogous to the option presented in *AutoGaitA_DLC,* which simulates all animals walking in the same direction. Finally, since having step cycle data for both legs, we implemented a way to analyse left and right leg separately. This means that all the user-defined kinematic features and corresponding plots are individually computed for the left and the right body side, with the output of the analysis stored in separate *Results* subfolders. These features are particularly important in the clinical settings because by minimizing the time spent walking to achieve sufficient trials, as both directions can be included, and by allowing to independently analyse left and right side of the body, which in certain disease, e.g. hemilateral stroke, can be differentially perturbed, make gait analysis more implementable for the general assessment of healthy individuals and patients.

Automated assessment of intergroup effects with AutoGaitA_Group

AutoGaitA_Group can only perform a series of group-level analyses, after the first-level algorithms (*AutoGaitA_DLC* or *AutoGaitA_Simi*) have generated and stored data in the *Results* folders. The analyses conducted by *AutoGaitA_Group* commence with the generation of group-level Excel files, which provide average and standard deviation data from all original and normalised step-cycles across each experimental group. Next, users can choose how to statistically compare the entire datasets across groups or selected features, by selecting cluster-extent permutation test, two-way analyses of variance (ANOVAs) or both (see also *AutoGaitA_Group's Statistical Procedures*). To visualise how kinematic features parse data in multidimensional space, *AutoGaitA_Group* includes a Principal Components Analysis (PCA). *AutoGaitA_Group* generates excel and/or text files containing the results of the statistical comparisons and the PCA, including

the exact time-bin ranges of statistically significant clusters if present or the percentage of explained variance and eigenvectors for all PC. Finally, it also produces figures representative of the group analysis (as *png* or *svg* formats), e.g. ankle angle's averages per step cycle per group or results of the statistical comparison (statistically significant bins highlighted by a light red background). PCA results are visualised with 2D and 3D scatterplots, with users having the option to save the rotating 3D scatterplot as video file (see also *Detailed User Workflow*).

Showcase 1: Perturbation- and age-dependent changes in mouse 2D locomotor kinematics.

To test the efficacy and sensitivity of our toolbox in detecting kinematic changes, we designed a locomotor paradigm in which 9-week-old C57BL6/J untrained mice are tasked with crossing beams of different widths (25, 12 and 5 mm) (Gatto *et al.*, 2021). Mice are challenged to cross on day one the wide beam (25 mm) (**Figure 2A, left** and **Supplemental Video S1**), on day two the narrower beam (12 mm) (**Figure 2A, middle** and **Supplemental Video S2**), and on day three the narrowest beam (5 mm) (**Figure 2A, right** and **Supplemental Video S3**). The increasing difficulty encountered by mice in performing the tasks is indicated by the higher number of slips as beam width decreases (**Figure 2B**). This design allowed us to determine the flexible and rapid adaptation of gait to perturbations, and the underlying kinematic strategies. Prior to the analysis with *AutoGaitA_DLC,* we determined some baseline gait features that are essential to interpret the observed kinematic differences, i.e. the hindlimb stride duration and the percentage of time spent in swing within each stride. Calculating the swing duration is important to determine whether the observed kinematic differences indicate adaptive changes or just a change in the timing of swing-to-stance transition. We observed that mice sped up by shortening their stride duration when walking on the 12 mm beam, and slowed down by increasing their stride duration when crossing the 5 mm beam (**Figure 2C**). Similarly, the swing phase became significantly longer on the 12

mm beam, and significantly shorter on the 5 mm beam (**Figure 2D**). Taken together these results suggest that mice feel more at ease crossing the 12 mm beam, since they got used to the task on the previous day (25 mm beam crossing) and the beam width is not challenging enough.

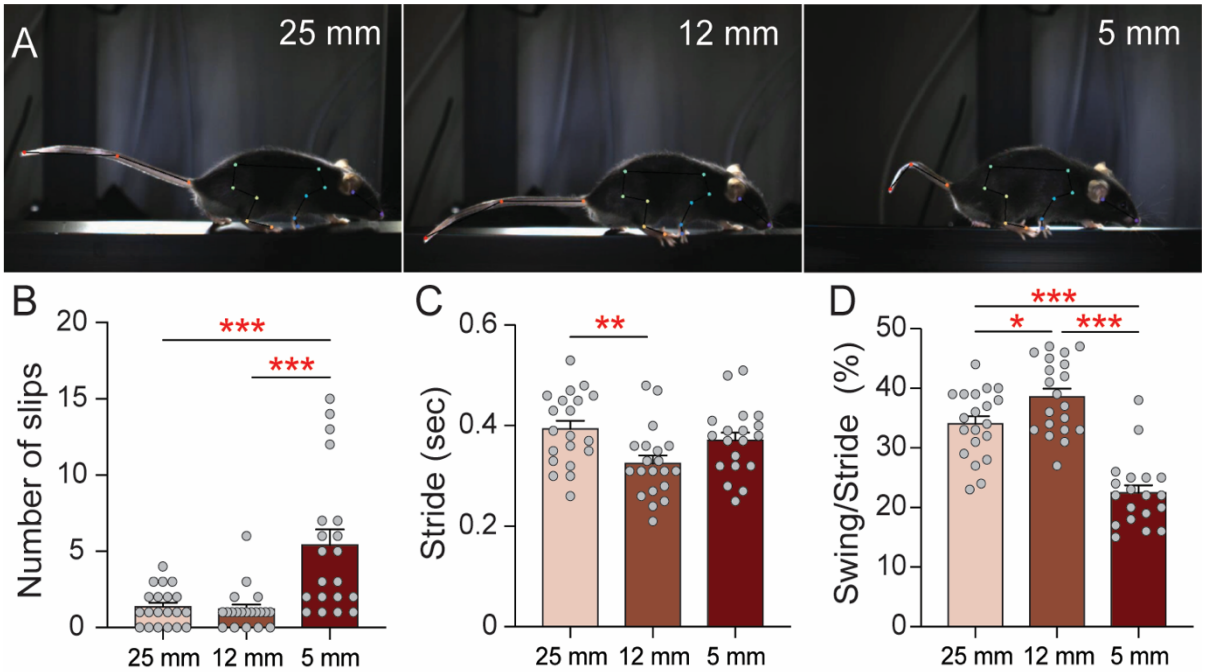

Figure 2. Beam width-induced slips and alteration to stride and swing duration. *A) Snapshots of mice crossing beams of increasingly narrower widths.* ***B****) Bar graph showing increased number of slips on the 5 mm beam.* ***C****) Decreased stride duration in mice crossing the 12 mm beam.* ***D****) Time spent in swing during a stride increases on the 12 mm beam and decreases on the 5 mm beam. Data are presented as mean±SEM, individual mice are represented as grey circles. Statistical significance was calculated with one-way ANOVA followed by Tukey's post-hoc test, with * p<0.05, ** < 0.01, *** <0.001*

Next, we used *AutoGaitA_DLC* to analyse 177 videos, corresponding to 20 mice running across the 25 and 12 mm beams for 3 trials, and 19 mice crossing the 5 mm beam for 3 trials. Using *AutoGaitA_Group,* we averaged kinematic features across groups and statistically compared beam width-induced changes with both cluster-extent permutation and two-way ANOVA tests (see also *AutoGaitA_Group's Statistical Procedures*). Results of the two-way ANOVA test were confirmed in GraphPad Prism as a further quality check. Further, the aesthetic of image vector figures generated by *AutoGaitA* (shown in *Detailed User Workflows*) were further optimized and customised for optimally showing the kinematic changes across tasks.

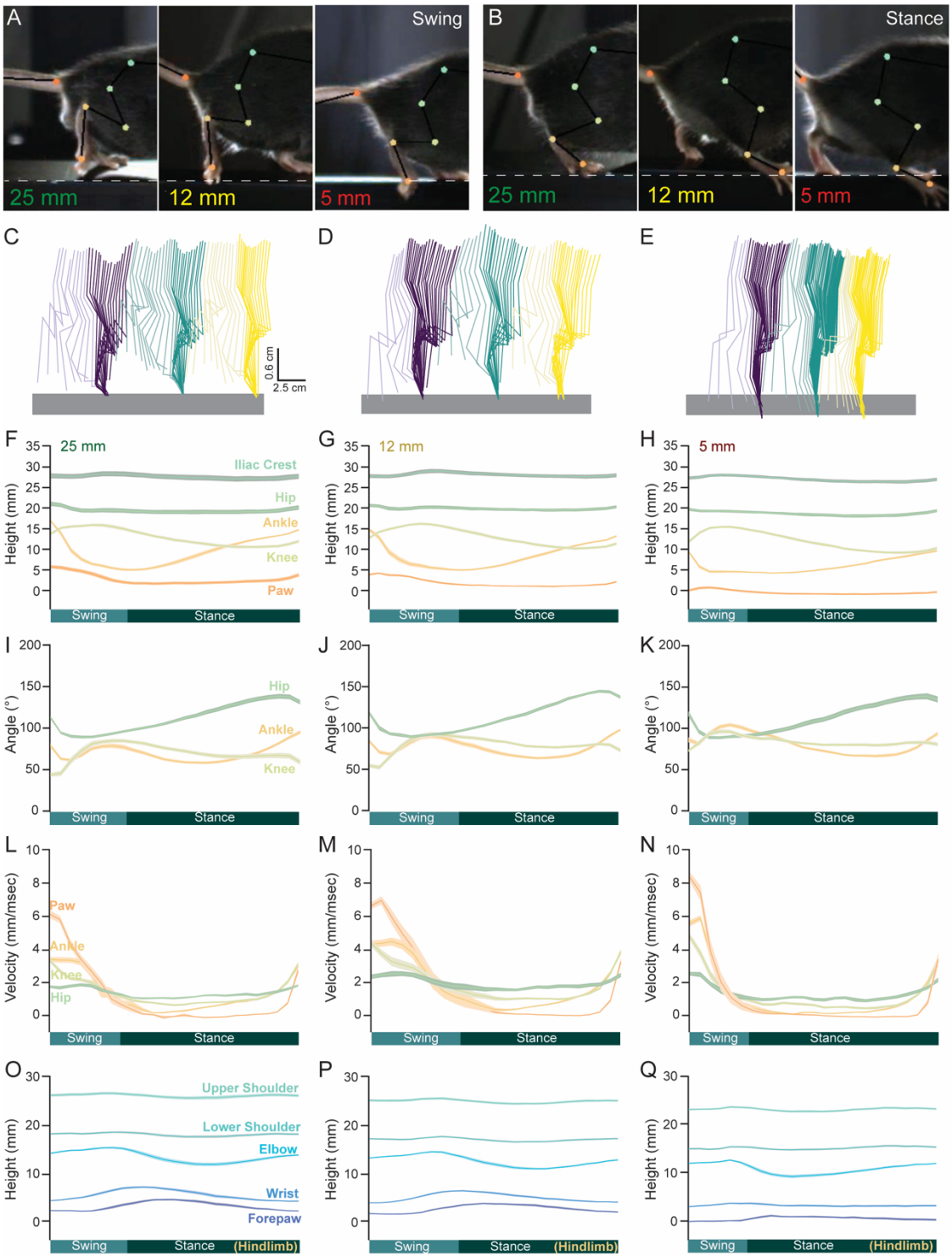

Figure 3. Beam width-induced changes in kinematics. A,B*) Snapshots showing the position of hindlimbs relative to the beam during swing (**A**) and stance (**B**) as mice cross increasingly narrower beams. **C-E**) Stick diagrams representing hindlimb vertical and horizontal position during swing (lighter lines) and stance (darker lines) in 3 consecutive steps of mice crossing 25 mm (**C**), 12 mm (**D**) and 5 mm (**E**) beams. Height (y-coordinate) of individual hindlimb joints (**F-H**), angles (**I-K**), velocity of each hindlimb joint (**L-N**) and height (y-coordinate) of individual forelimb joints (**O-Q**) during a normalised step cycle on the 25 mm (**F,I,L,O**), 12 mm (**G,J,M,P**) and 5 mm (**H,K,N,Q**) beams. Swing and stance are based on the hindlimb step cycle. Data are presented as mean±SEM, with mean indicated by a darker line and SEM as shaded areas.*

A first inspection of videos (**Figure 3A,3B**), stick diagrams (**Figure 3C-3E**) and joint height (**Figure 3F-3H**) showed a downward shift of the hindlimb positioning relative to the beam induced by the narrowing of the beam width. During swing on narrower beams mice lifted their hindlimbs less, with the midfoot kept closer to the beam (**Figure 3A,3C-3H**). During stance, as beam width decreased, mice shifted their hindlimb placement from the top of the beam to the side, with the hindlimb still being clung to the beam by the toes but positioned below rather than on the beam surface (**Figure 3B-3H**). The second kinematic change is the relative position of the ankle compared to the knee. On the wider beams, the ankle is raised above the knee at the beginning of swing and end of stance, while on the 5 mm beam it remains below the knee for the entire step cycle (**Figure 3F-3H**). Comparing the angles, we observed that the angular excursion decreased as the beam width narrowed and angles were wider, indicating the limb was more extended (**Figure 3I-3K**), as also shown by the stick diagrams (**Figure 3C-3E**). The velocities of individual joints follow a distal-to-proximal order, with the hindpaw moving faster than the hip at the beginning of swing. The reduction of the beam width caused an increase in the speed of individual joints at the beginning of swing (**Figure 3L-3N**). Individual joints decelerated at the beginning of swing and accelerated at the end of stance, still following the distal-to-proximal order (**Figure S1A-S1C**). Finally, angular velocity of the ankle peaked mid-swing and end of stance, of the knee mid-swing, and of the hip mid-stance (**Figure S1D-S1F**). Ankle and hip angular acceleration peaked mid-swing and decreased end of stance, while knee angular acceleration decreased at beginning of swing and end of stance (**Figure S1G-S1I**). Finally, similar to hindlimb positioning, the y-coordinates of the forelimb showed a significant downward shift of the joints as beam width narrowed (**Figure 3O-3Q**).

Next, we statistically tested differences in individual kinematic features across beams using *AutoGaitA_Group* (see also *Detailed User Workflow*) to confirm the presence of an adaptation signature. When mice cross the narrowest beam (5 mm) the body was kept closer to the walking surface and individual distal joints were significantly lower during both stance and swing (**Figure 4A-4C**, significance across beam pairs is indicated by red (25 vs 5 mm), yellow (12 vs 5 mm) and green (25 vs 12 mm) asterisks). Differences in the height of limb positioning between the 25 and 12 mm beams were observed for the very distal joints, i.e. hindpaw and ankle (**Figure 4A,4B**), and less so for the proximal hip and iliac crest (**Figure S2A,S2B**). During the swing phase on the 5 mm beam, the ankle and knee but not hip formed wider angles, whereas during stance the ankle was less flexed and the knee more extended (**Figure 4D-4F**). As described for the hindlimb, the position of individual forelimb joints also got closer to the beam as beam width narrowed (**Figure 4G-4I** and **S2C,S2D**). As beam width decreased, velocities of all joints (**Figure 4J-4L** and **S2E,S2F**) increased at the beginning of swing to minimise the time the hindpaw spent not in contact with the beam (**Figure 4J-4L**). Individual joints displayed a higher deceleration at the beginning of swing on the narrower beams (**Figure 4M-4O**). On the 5 mm beam, the decrease in angular velocity of the ankle was faster and appeared earlier in mid-swing (**Figure 4P**), whereas knee and hip angular velocities showed changes at both beginning of swing and end of stance (**Figure 4Q, 4R**). Changes in angular accelerations followed similar trends (**Figure S2G-S2I**).

Next, we used *AutoGaitA_Group* to run a Principal Components Analysis (PCA) on all the analysed kinematic features (hindlimb height, angles, velocities, acceleration, and forelimb height) to compare gait across beams, which divides the data into 3 clusters in two-dimensional principal component (PC) space, each corresponding to a specific beam width (**Figure 5A**). The separation across tasks was even more evident in a three-dimensional PC space (**Figure 5B**).

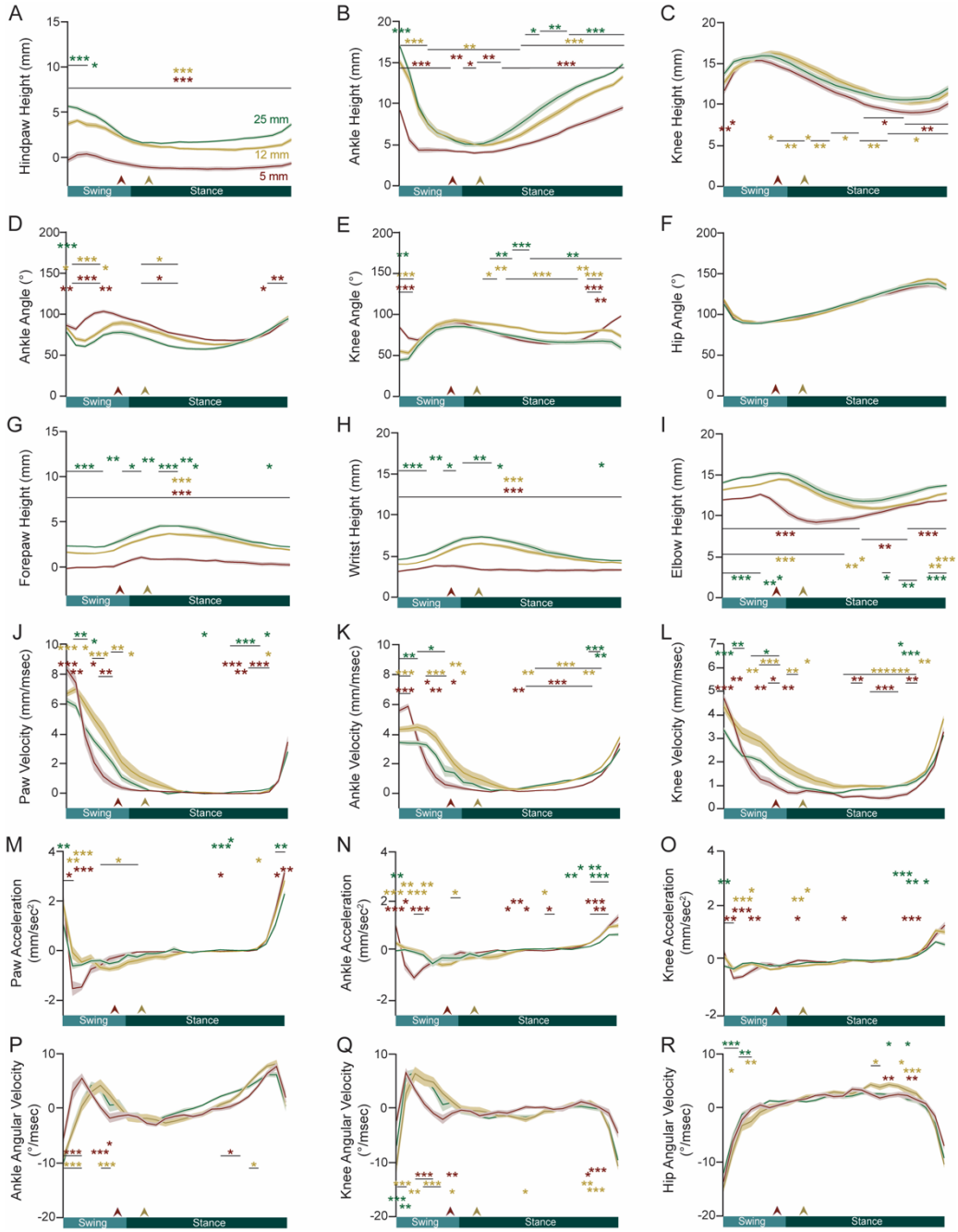

Figure 4. Kinematics of beam adaptation. *A-C) Changes in height (y-coordinate) of hindpaw (**A**), ankle (**B**) and knee (**C**) as mice cross the 25 mm (green), 12 mm (yellow) and 5 mm (red) beams. **D-F**) Changes in ankle (**D**) and knee (**E**) but not hip (**F**) angle as mice are challenged with different beams. **G-I**) Beam width-induced changes in height (y-coordinate) of forepaw (**G**), wrist (**H**) and elbow (**I**). **J-L**) Changes in hindpaw (**J**), ankle (**K**) and knee (**L**) joint velocity. **J-L**) Changes in hindpaw (**J**), ankle (**K**) and knee (**L**) joint velocity. **M-O**) Beam width-induced changes in hindpaw (**M**), ankle (**N**) and knee (**O**) joint acceleration. **P-R**) Beam width-induced changes in ankle (**P**), knee (**Q**) and hip (**R**) angular acceleration. Data are presented as mean±SEM, with mean indicated by a darker line and SEM as shaded areas. The yellow and red arrowheads indicate the swing duration when mice cross the 12 and 5 mm beams, respectively. Statistical significance was calculated with a two-way ANOVA followed by Tukey's post-hoc test, 25 mm vs 5 mm (red asterisks), 12 mm vs 5 mm (yellow asterisks), 25 mm vs 12 mm (green asterisks).*

PC1 was predominantly defined by knee and ankle angles during swing, PC2 by knee and ankle angles during stance, and PC3 by joint velocities and accelerations (see percentage of explained variance in supplemental *PCA_5A_Table*). We also tested whether a reduced set of parameters was sufficient to parse out the gait on the three beams in a two-dimensional PC space. Thus, we performed PCA using only height of hindlimb and forelimb joints and hindlimb angles, the features most sensitive to the beam width, and showed that they were sufficient to identify beam width-specific clusters (**Figure 5C**). In this case, PC1 was mostly defined by knee and ankle angles, while PC2 by the height of forepaw and hindpaw (see supplemental *PCA_5C_Table*).

Finally, PCA is also extremely useful in comparing the kinematic features of adaptation across groups, like mice of different ages (3 months, 9 months, and 24 months) crossing the different beams (**Figure 5D-E**). In the two-dimensional PCA comparison across beams and ages (**Figure 5D**), the PC are the same as described in **Figure 5C** (see supplemental *PCA_5D_Table*). In older mice the separation of groups in three-dimensional PC space becomes more clear, and individual age/beam groups can be easily identified as distinct clusters (**Figure 5F** compared to **Figure 5E**). In the three-dimensional PC comparison between 3-month- and 9-month-old mice, PC3 is represented by hindpaw and ankle height (**Figure 5E**, see supplemental *PCA_5D_Table*). In the three-dimensional PC space separating 3-month- and 12-month-old mice, PC1 represents mostly the shoulder and elbow height, PC2 the ankle and wrist height, and PC3 the hindpaw and ankle height (**Figure 5F**, see supplemental *PCA_5F_Table*).

In summary, in this showcase, we presented a comprehensive dataset generated using *AutoGaitA,* and demonstrated how the extracted kinematic features can be used to compare the same mice performing different tasks (**Figures 2-5**) or diverse groups of mice across tasks (**Figure 5**). In our example dataset, we introduced strong perturbations (5 mm beam) and extreme ageing

(24 months), therefore we observed many significant kinematic changes across groups. For more subtle mutations or manipulations of neural activity, the number of features analysed and used for PCA might be higher or lower depending on the experimental conditions and the expected motor impairments.

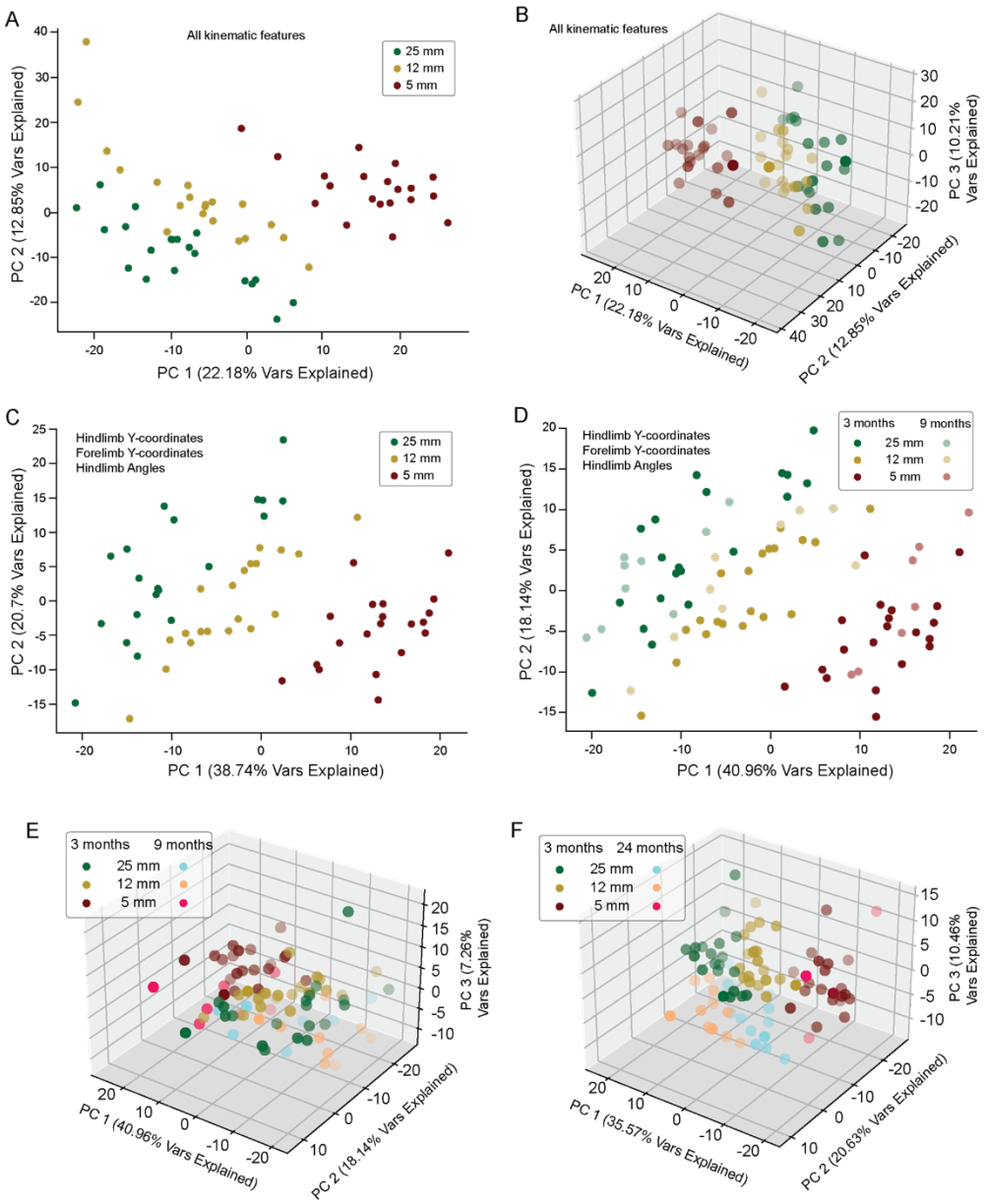

Figure 5. PCA of locomotor gait across beams and ages. A,B) *PCA using all kinematic features extracted in two-dimensional* ***(A)*** *and three-dimensional* ***(B)*** *principal component space.* ***C)*** *PCA using only hindlimb and forelimb y-coordinates as well as hindlimb angles identifies 3 separate clusters.* ***D,E,F)*** *PCA analysis of all analysed kinematic features comparing 3-month-old with 9-month-old* ***(D,E)*** *and 24-month-old* ***(F)*** *mice in two-* ***(D)*** *and three-dimensional* ***(E,F)*** *principal component space.*

Showcase 2: Age-dependent changes in humans and mice.

To verify that *AutoGaitA* is compatible with the output of other tracking algorithms and can extract features in a similar manner across species, we developed a gait paradigm in healthy subjects to assess the effects of ageing in humans. Young adults (21 to 35 years) and elderly human participants (65 to 85 years) were asked to self-paced walk on a 60 cm wide runway while being filmed using 8 high-speed cameras. Simi Shape (Winiarski, 2003) was used to track joint and landmark coordinates in 3D from individual videos, and coordinates were analysed using *AutoGaitA_Simi* (**Figure 6A**) (see also the *Detailed User Workflows*). To have an age-matched cross-species comparison, we used 9-month- (adult) and 24-month-old (elder) mice walking on a 25 mm beam (**Figure 5,** *Showcase 1*).

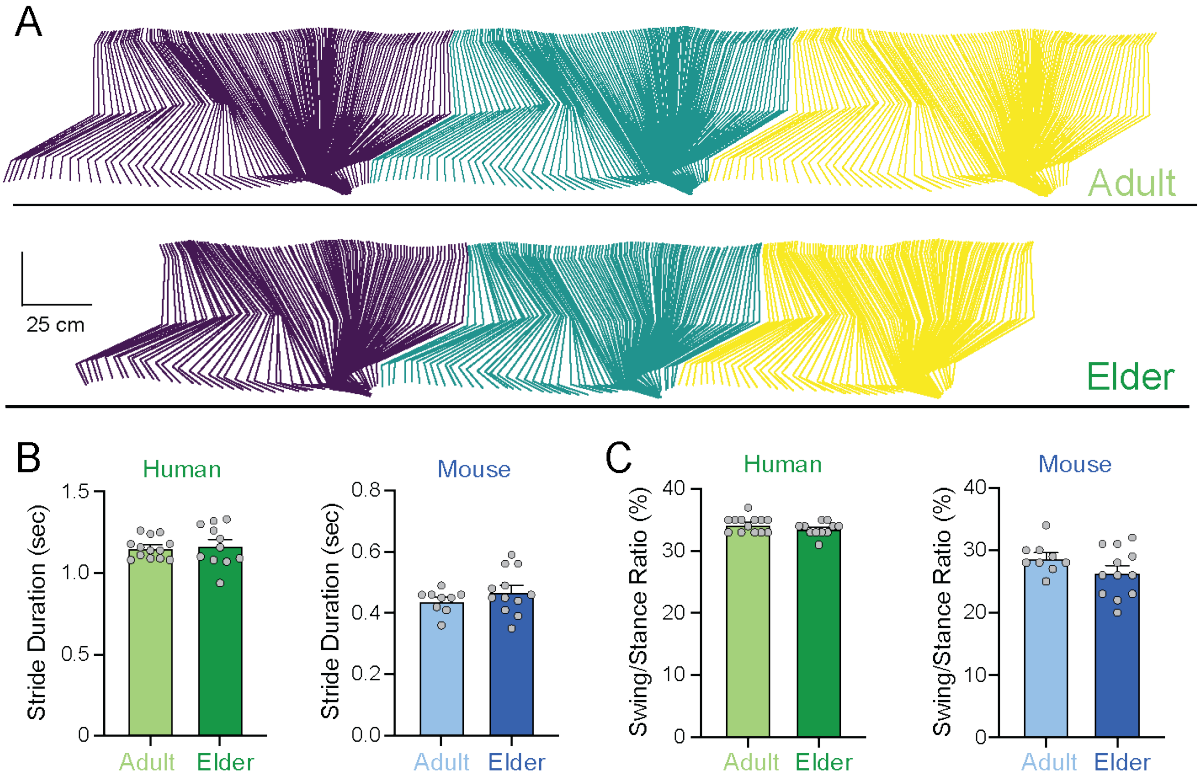

Figure 6. Age-dependent changes in stride features in humans and mice. A) *Stick Diagram of human leg locomoting.* ***B,C)*** *Bar graphs showing the absence of significant age-induced changes in stride duration* ***(B)*** *and swing/stance ratio* ***(C)*** *in humans and mice. Statistical significance was calculated with unpaired two-tailed Student's t-test.*

We started by analysing changes in stride duration and the ratio of time spent in swing and stance phases. In both mice and humans, age did not significantly change the duration of stride (**Figure 6B**) nor the ratio of swing to stance within each stride (**Figure 6C**). Next, we assessed how height of the leg joints, angles and velocity change in humans and mice with age. Ageing mildly affected human foot lift, making it less pronounced towards the end of swing, with ankle and midfoot being closer to the ground, but no significant changes in knee and hip height (**Figure 7A,7C,7E,7G**). Notably, the effect was more pronounced on the right than the left leg (**Figure 7A,7C,7E,7G** and **S1A-S1D**), which can denote either some differences between the dominant and non-dominant side of the body or the need to enlarge our

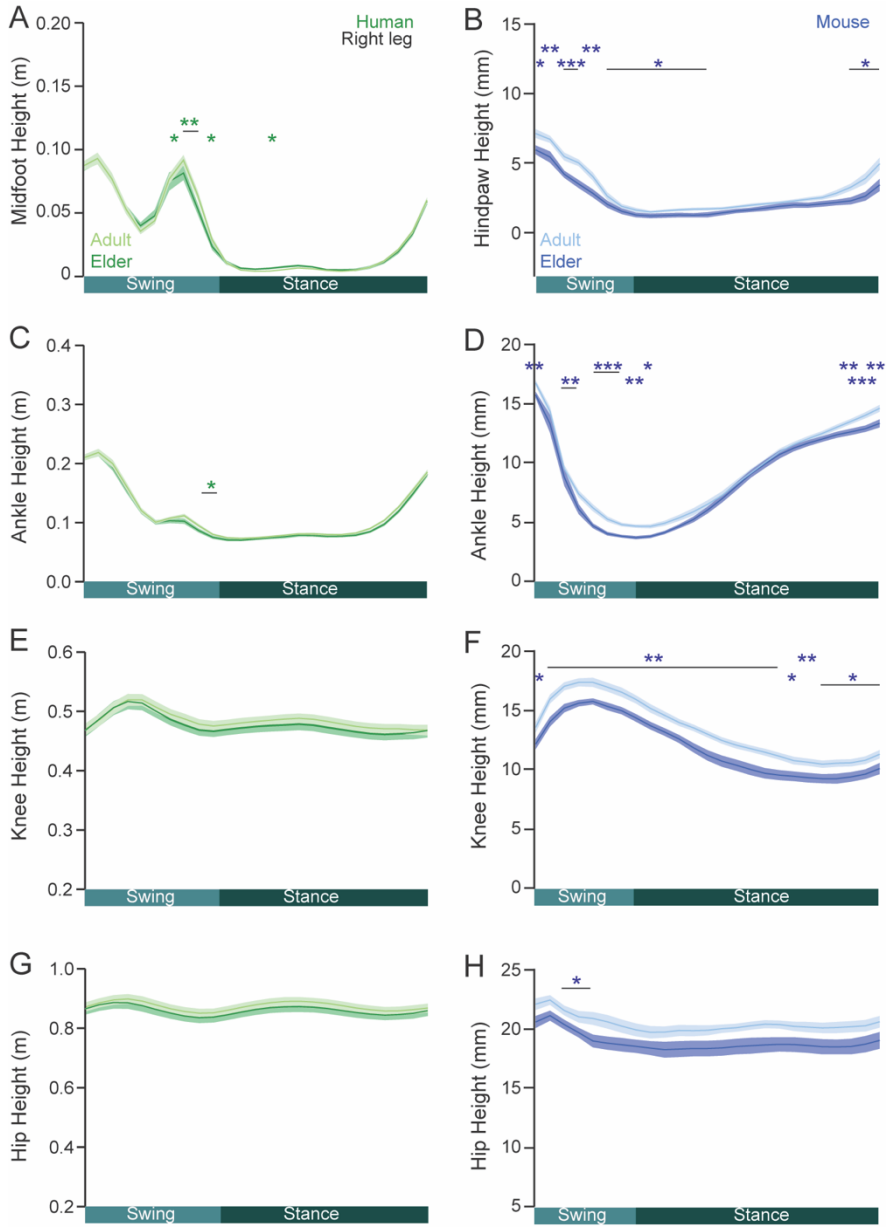

Figure 7. Age-dependent changes in height of individual joints in humans and mice. *Changes or lack thereof in vertical position (z-coordinate in humans, y-coordinate in mice data) of midfoot/hindpaw (**A,B**), ankle (**C,D**) knee (**E,F**) and hip (**G,H**) of humans (**A,C,E,G**) and mice (**B,D,F,H**) Statistical significance was calculated with a two-way ANOVA followed by Tukey's post-hoc test.*

dataset due to higher interindividual variability. By contrast, older mice significantly lowered their joint heights, predominantly during the swing phase (**Figure 7B,7D,7F,7H**). Hip and knee angles were mostly unchanged in both species (**Figure 8A-8F**), but older mice displayed a significant decrease in their ability to flex the ankle between mid-swing and mid-stance periods (**Figure 8B**). Human hip, knee, ankle and midfoot moved significantly slower during swing, with the additional slowdown of knee, ankle, and hip movement velocities also during stance (**Figure 9A,9C,9E,9G**). Joint velocities in mice were only partially affected, with hip and ankle minorly slowing down during swing (**Figure 9B,9D,9F,9H**).

Taken together, our data show that ageing in healthy mice and humans causes convergent and divergent changes in locomotor kinematic features in unperturbed conditions. Stride duration and swing/stance ratio were preserved in both species. Both humans and mice showed a reduced height of their foot (paw) and ankle at the end of swing. By contrast, older mice kept their entire body

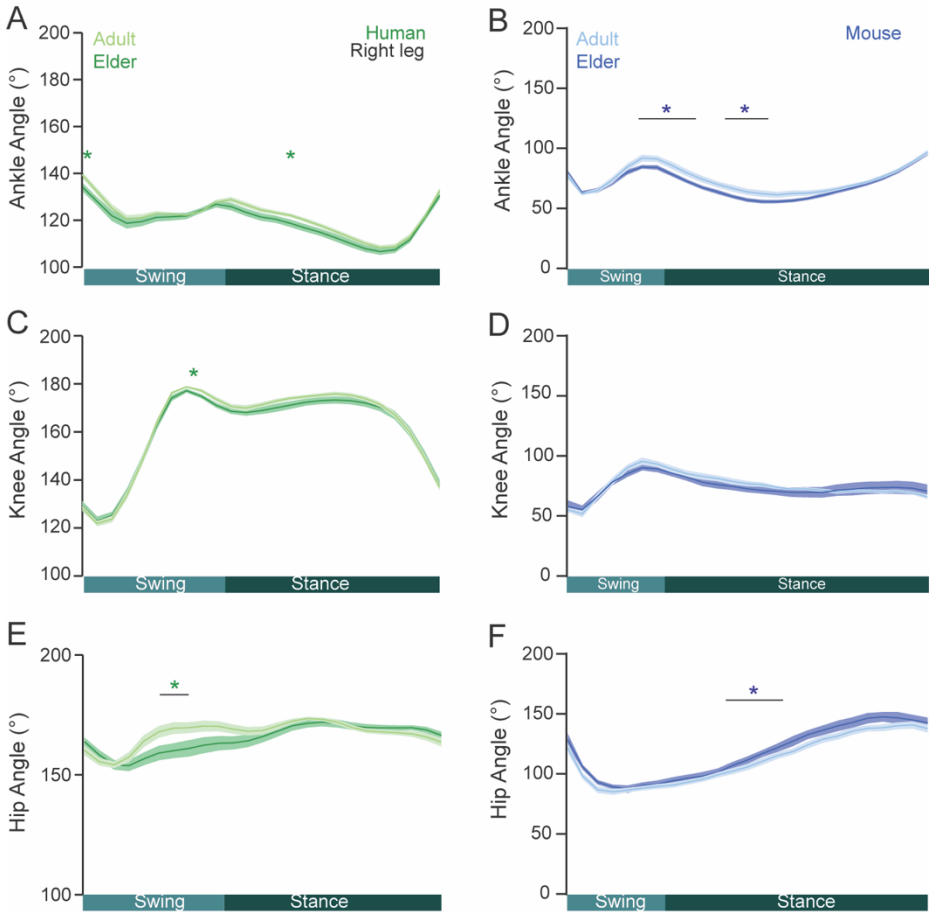

Figure 8. Age-dependent changes in angles in humans and mice. *Changes or lack thereof in ankle (**A,B**), knee (**C,D**) and hip (**E,F**) angles of humans (**A,C,E**) and mice (**B,D,F**). Statistical significance was calculated with a two-way ANOVA followed by Tukey's post-hoc test*

closer to the floor, by lowering all the joints during swing, and reducing the paw, ankle and knee height also during stance. Angles changed in different ways between the two species, with older human subjects having a wider hip angle during swing, whereas older mice had a more flexed hip angle during mid-stance and a wider ankle angle from end of swing to mid-stance. Effects on joint velocities were more pronounced in humans, with distal joints slowing predominantly during swing, and proximal joints being slower during both swing and stance. In sum, humans predominantly slow down to minimize age-induced uncertainties in gait, while mice preferentially lower their centre of mass.

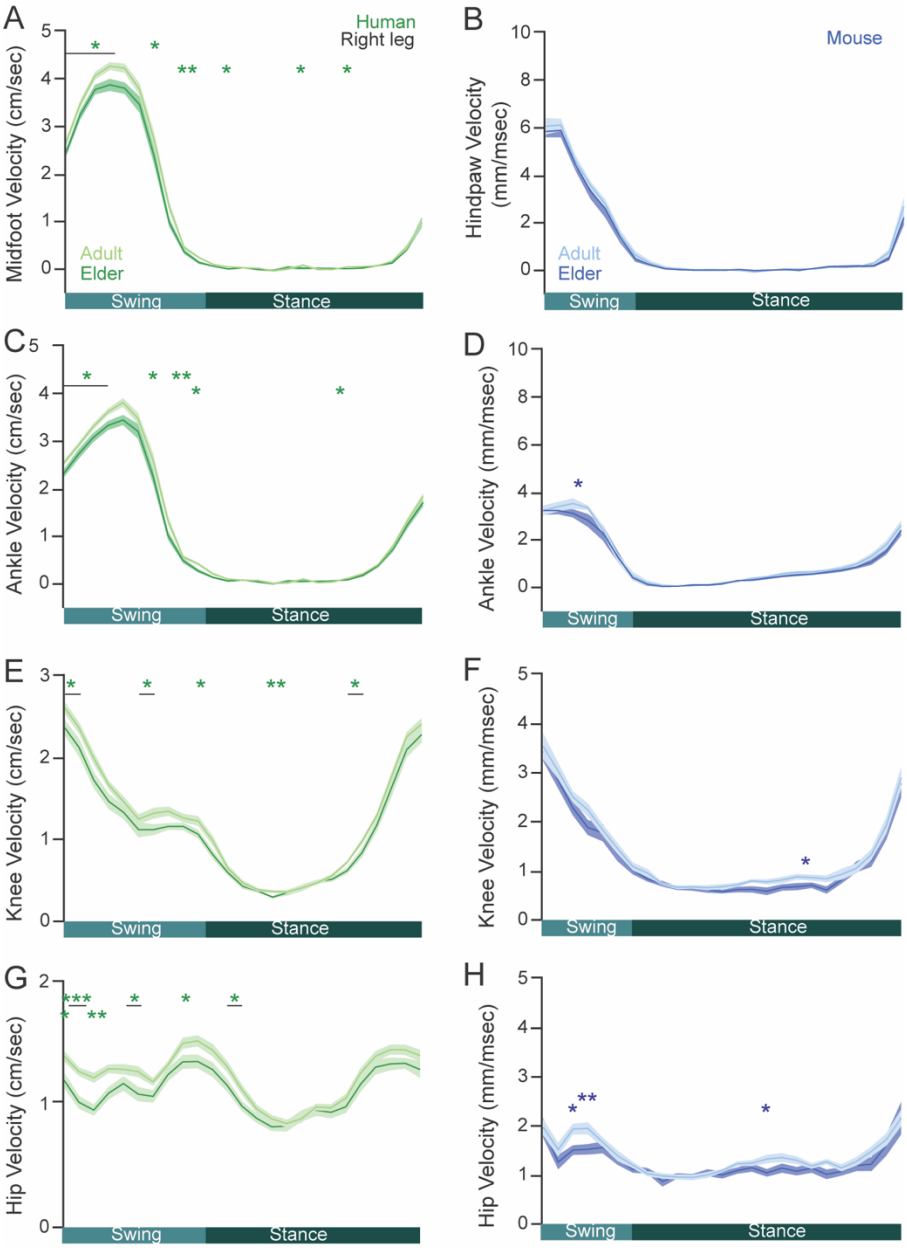

Figure 9. Age-dependent changes in joint velocities in humans and mice. *Changes (or lack thereof) in midfoot/hindpaw (**A,B**), ankle (**C,D**) knee (**E,F**) and hip (**G,H**) joint velocities in humans (**A,C,E,G**) and mice (**B,D,F,H**). Statistical significance was calculated with a two-way ANOVA followed by Tukey's post-hoc test.*

Showcase 3: Cross-species Comparison.

Finally, we demonstrate *AutoGaitA's* capacity to analyse locomotion in another species, *Drosophila*, comparing adult vs. old animals. Flies walked on a ball and the coordinates were tracked using DLC. *AutoGaitA*'s joint and angle customisation feature allowed us to run our standardised analysis even in a different species, in which key points are indicated with specific nomenclature, e.g. FiTar (fibula-tarsum) rather than knee. This feature of *AutoGaitA* enables the analysis of any joint or angle *in general*, irrespective of species or behaviour.

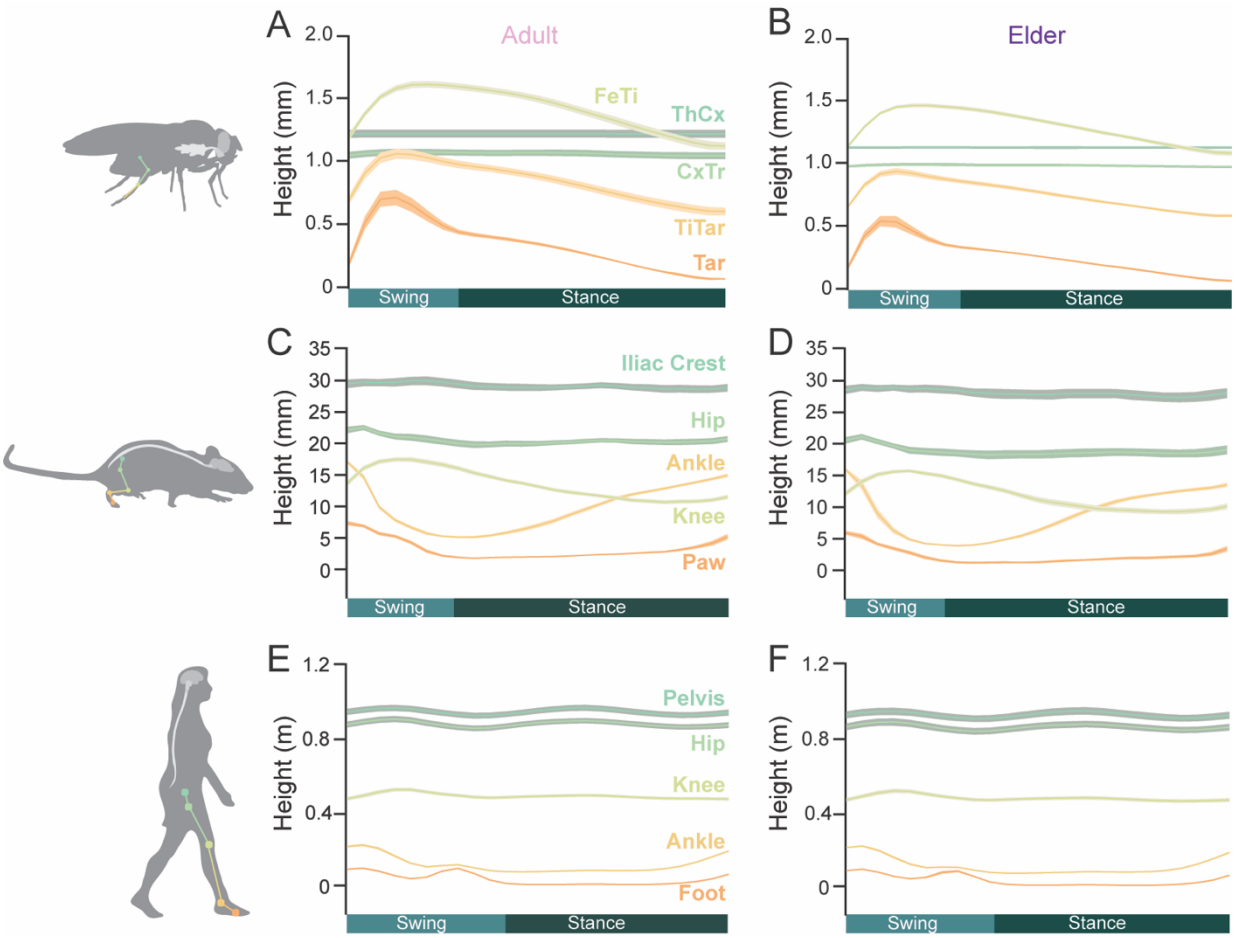

Figure 10. Joint heights in adult and old flies, mice and humans. *Vertical position (y-coordinate in flies and mice, z-coordinate in humans) of Tar/hindpaw/midfoot, TiTar/ankle, FeTi/knee, CxTr/hip and ThCx/iliac crest/pelvis of adult (**A,C,E**) and old (**B,D,F**) flies (**A,B**), mice (**C,D**) and humans (**E,F**).*

We used *AutoGaitA_DLC and AutoGaitA_Group* to analyse the fly data and compare the kinematic features across species. We tracked 5 joints: the Thorax-Coxa (ThCx), the Coxa-

Trochanter (CxTr), the Femur-Tibia (FeTi), the Tibia-Tarsus (TiTar) and the Tarsum (Tar). The height measure of joints/key points showed that the proximal CxTr joint (corresponding to the hip in mice/humans) is kept at a steady height in flies, is minorly deflected down at the beginning of swing in mice and acts as a pendulum in humans (**Figure 10**). The FeTi/knee joint shows ample vertical excursions in flies and mice, but limited vertical movements in humans, mostly limited to the swing phase (**Figure 10**). Both mice and humans showed two peaks in paw/foot height during swing, one corresponding to the flexion to lift, and the second to the targeting (forward propulsion) phase (**Figure 10**). Yet, as animals aged, the relative position of their joints was preserved, with flies and mice showing a more prominent lowering of their body towards the floor in both swing and stance phases (**Figure 10**, see also **Figure 7**).

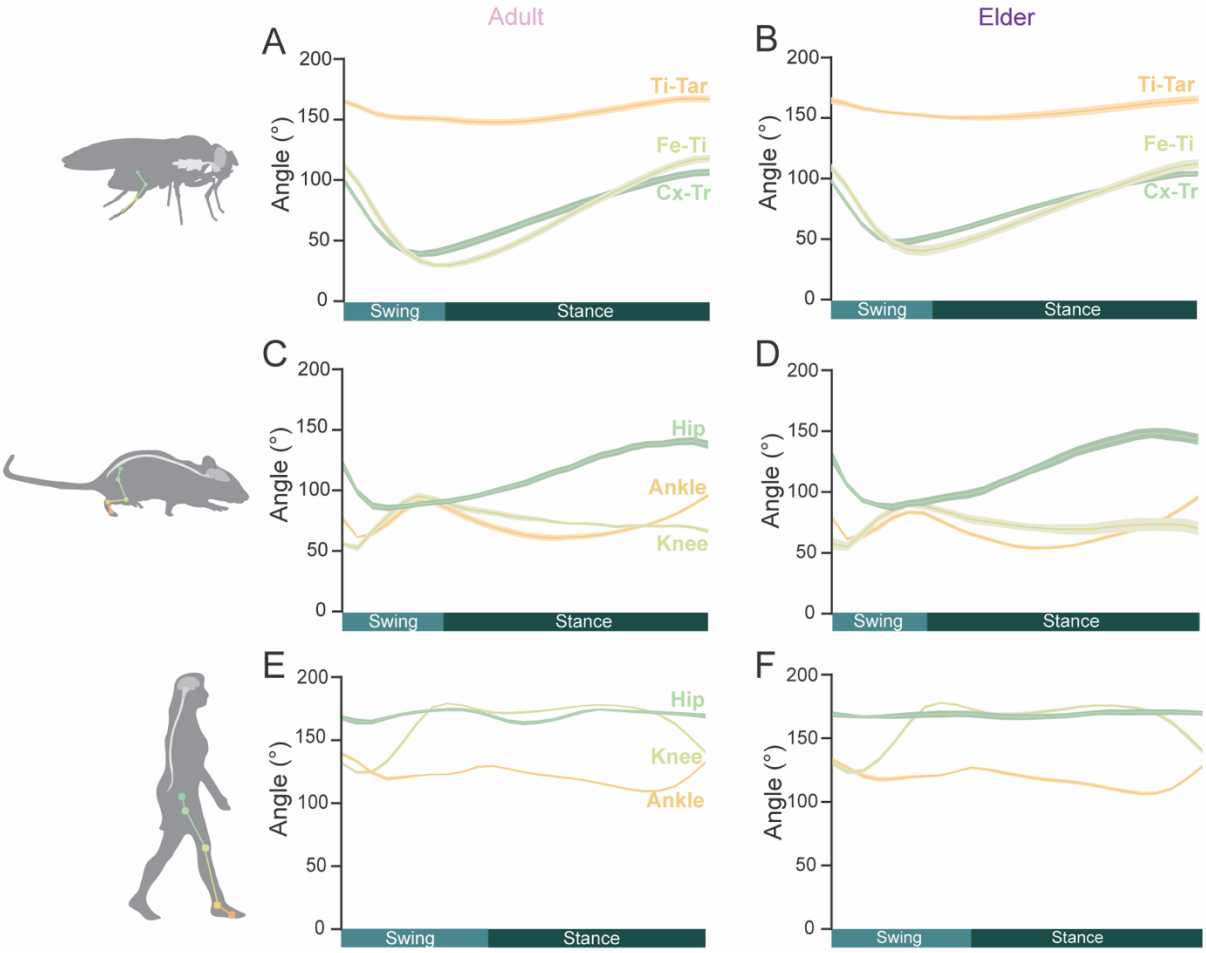

Figure 11. Angles in adult and old flies, mice and humans. *Ti-Tar/ankle, Fe-Ti/knee, Cx-Tr/hip angles of adult (**A,C,E**) and old (**B,D,F**) flies (**A,B**), mice (**C,D**) and humans (**E,F**).*

The angles that change in similar ways during the step cycles are different across species, in flies Fe-Ti (knee) and Cx-Tr (hip) angles, in mice knee and ankle angle, and in humans ankle and hip angles (**Figure 11**). These patterns of angular coordination do not change with ageing (**Figure 11**).

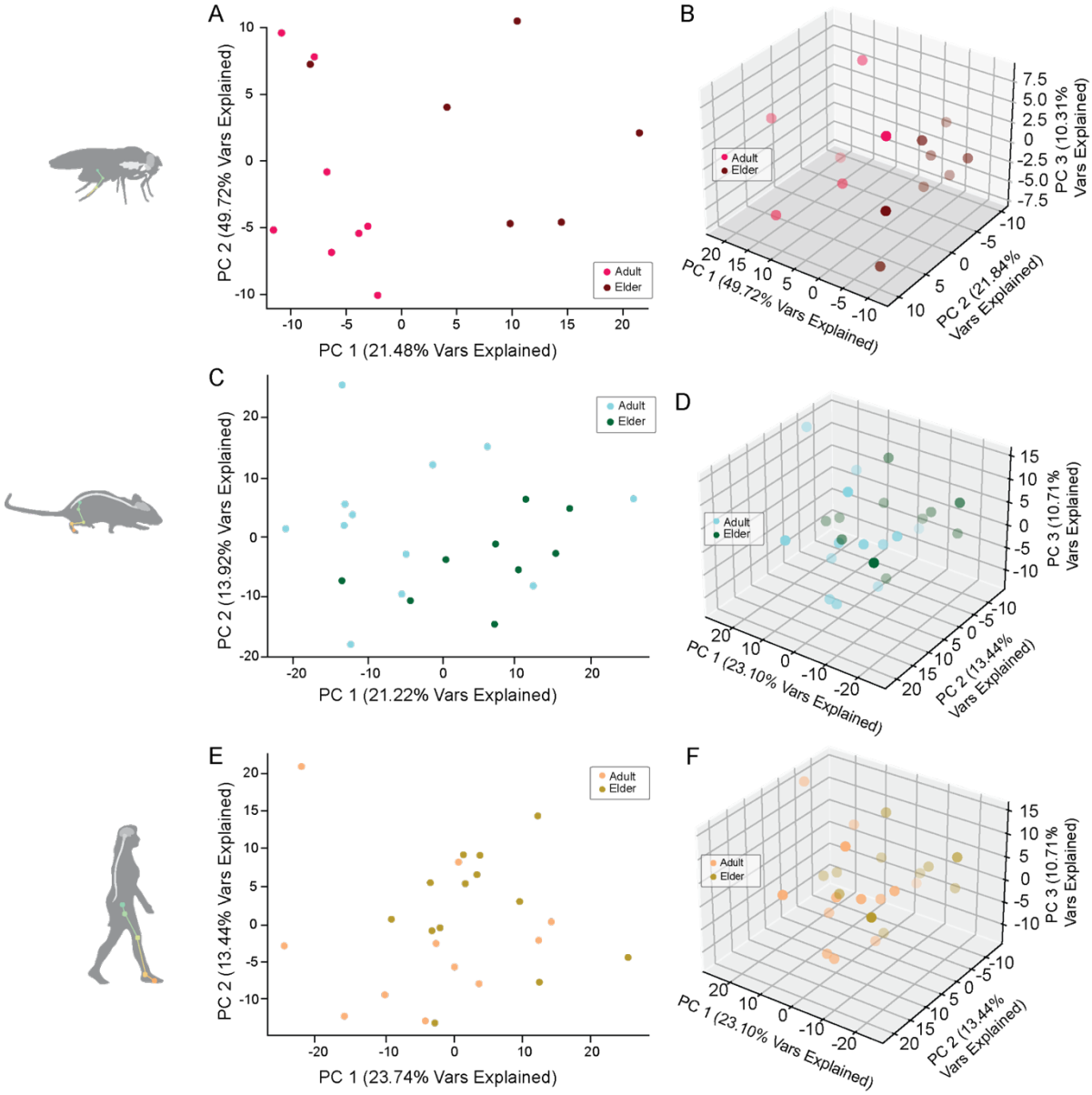

Figure 12. ***PCA of locomotor gait across species and ages*** **(A-F).** PCA using all kinematic features extracted in two-dimensional **(A,C,E)** and three-dimensional **(B,D,F)** principal component space in flies **(A,B),** mice **(C,D)** and humans **(E,F)**. Note that these figures present results of three separate (species-specific) PCAs, generated using the same input features.

Finally, using all the analysed kinematic features for PCA analysis, age-dependent clusters were clearly separated in flies and less so in mice and humans, probably due to humans mostly changing the speed at which the individual joints move as they age, while flies and mice changed more parameters (**Figure 12, and *PCA_Table_Cross-species***). In flies, PC1 is predominantly due to height of Ti-Tar and Cx-Tr joints, PC2 to Tar and Fe-Ti height, and PC3 to Th-Cx height and Fe-Ti angle (see *Fly Tab* in ***PCA_Table_Cross-species***). In mice, PC1 is predominantly due to iliac crest, hip, and knee height, PC2 to knee and hip angle, and PC3 to shoulder height and ankle angular velocity (see *Mouse Tab* in ***PCA_Table_Cross-species***). Finally, in humans PC1 is predominantly due to ankle, knee and hip height, PC2 to ankle, knee and hip velocity, and PC3 to foot, midfoot and ankle height (see *Human Tab* ***PCA_Table_Cross-species***).

In summary, we used our new toolbox to compare age-induced in locomotor kinematics across species. We could show that age changes the gait of different animals, but it does so by affecting kinematic features in a species-specific fashion.

Discussion

We developed *AutoGaitA*, an open-source Python toolbox to automate the study of locomotion (and other rhythmic behaviours) after body posture tracking with DLC (Mathis et al., 2018) and Simi Shape (Winiarski, 2003). We further showcased three experimental applications, demonstrating how *AutoGaitA* automated the gait analysis of fly, mouse, and human data after ML-based body tracking and how *AutoGaitA_Group* enabled comparisons across age groups, tasks (e.g., beam width) or species. In sum, *AutoGaitA* provides a simplified and standardised analysis of locomotion, yet further implementations are planned to expand capabilities and

overcome limitations in the current *AutoGaitA* beta version (https://github.com/mahan-hosseini/AutoGaitA).

Expanding the repertoire of kinematic features and behaviours

AutoGaitA was developed with the goal of automating gait analysis, i.e., locomotion in walking vertebrates. We used *AutoGaitA* to assess walking in flies, mice and humans, focusing on hindlimb features, which in our paradigm were sufficient to highlight some task- and age-dependent differences. Another study used *AutoGaitA* to assess kinematic changes as mice with cerebellar dysfunction were challenged to cross beams of different widths (Tutas et al., 2024). We implemented some degree of flexibility with users being able to customise joint names, angle definition (see the *Custom column names and features window* in the online documentation) or include more joints/key points and/or angles to the analysis and select the input values for PCA. Nevertheless, more features, such as horizontal coordinates, 3D reconstructions and interlimb coordination might be required to better address kinematic effects of targeted lesions (e.g. focal stroke lesions) or genetic mutations.

In this paper, we showcased the toolbox utility in detecting and comparing kinematic differences in mice performing three different tasks. Nevertheless, it should be emphasised that *AutoGaitA* can be used to automate the study of kinematics of flying or swimming, as well as reaching or rope pulling, or any other behaviour. For other behaviours, although the general workflow remains similar, the *Annotation Table* must contain the onset and offset latencies of the timepoints defining occurrences of the task assessed. For example, if users are interested in scratch behaviour, the *Annotation Table* will contain the time of the forward extension of the limb (ti) and the time of the backward flexion (te), rather than initiation of swing and stance. Features are then normalised, exported, plotted, and analysed via PCA and statistics, as shown for locomotion. Even

though *AutoGaitA* can be in theory used for any behaviour (the toolbox works independently of the meaning of the data), certain constraints do exist. For example, *AutoGaitA_DLC* can only be used on 2D data, and it should be stressed that the current analysis is optimised for a lateral view camera, as also shown in the showcase examples. Thus, users are advised to carefully consider how *AutoGaitA_DLC* computes features in the x/y plane before conducting their experiments using other views.

We expect *AutoGaitA* to reach the limitations of its capabilities in ways that we cannot yet foresee. As a result, feedback (to autogaita@fz-juelich.de) from users attempting to analyse different behaviours or videos from different angles is appreciated, so we can continue improving *AutoGaitA's* analysis flexibility in the future.

Species Independence and Cross-Species Comparisons

We named the first-level toolboxes *AutoGaitA_DLC* and *AutoGaitA_Simi* to emphasise that the algorithm used for body posture tracking is the main factor necessitating two distinct toolboxes, as their output files differ in terms of data structure. *AutoGaitA* has been developed and tested to read and analyse 2D kinematic features from 2D coordinates generated with DLC (locomotion data for mice and flies) and 3D coordinates obtained with Simi (human locomotion data). Nonetheless, our toolbox can analyse the kinematics of any species as long as users provide 2D data for *AutoGaitA_DLC*, and 3D data for *AutoGaitA_Simi*. To analyse other species, users only have to configure the column names of joints (or, more generally, keypoints) as well as define how angles should be computed (i.e., defining which three joints constitute a given angle).

AutoGaitA flexibility facilitates cross-species comparisons. As long as the same first-level algorithm (*AutoGaitA_DLC* or *AutoGaitA_Simi*) was used and analysis parameters match (e.g., same features of interest, sampling rate, etc.), users can easily use *AutoGaitA_Group* to analyse up

to six species with each other (see online documentation, particularly *sections E. and B. in autogaita.dlc_gui() and autogaita.simi_gui()*).

Future developments

Automatic Extraction of Step Cycle Times

AutoGaitA accelerates and standardises many key components of studying locomotion after body posture tracking via ML. It is stressed that the manual annotation of step cycle times and the generation of the Annotation Table provides the user with an important degree of flexibility and control. Keeping the input datasets themselves fixed (e.g., all included in their directory), users can easily change what is being analysed in a given run of our toolbox simply by changing the entries of the Annotation Table file. This allows users to, for example, only include steps before a mouse slipped or exclude the first and last steps of a human gait analysis. Nonetheless, we acknowledge that this preparatory step requires a substantial amount of effort and care. We have, therefore, been developing an extension to *AutoGaitA*, which aims to automatically identify and propose step cycle times after reading the data files generated by DLC and Simi. Even though our preliminary results look promising, further careful optimisation is required. Optimising our method requires a large number of datasets and Annotation Tables. We therefore appreciate users who would like to support us with this endeavour. To do so, users are encouraged to send us their (DLC or Simi) datasets alongside corresponding Annotation Tables to *autogaita@fz-juelich.de*.

Tool to reject bad step cycles

At present, removing (first-level) data of step cycles that are deemed too noisy or inappropriate for group analyses involves a re-run of the first-level toolbox after the steps' timestamps have been excluded from the Annotation Tables (see the *Preparation of Annotation Table files* section). We

acknowledge room for improvement in this procedure and are currently developing a way of rejecting step cycles before running *AutoGaitA_Group* in a more user-friendly manner.

Other Toolboxes

Deep learning (DL)-based approaches to body posture tracking and the study of motor control have seen a striking increase in popularity over the last years (see Luxem et al., 2023 for a review of open-source tools). Much work has been conducted to optimise the deep models and improve tracking capabilities, for example, facilitating multi-animal posture tracking (Pereira et al., 2022) and enabling the conversion of 2- to 3-dimensional poses (Gosztolai et al., 2021). Another line of research has focussed on using DL approaches for the classification of behaviour (Dunn et al., 2021; Nilsson et al., 2020; Weinreb et al., 2023). With respect to kinematic analyses, some important tools have been introduced as well. However, they have so far all focussed on specific species (Aljovic, 2022; Karashchuk et al., 2021) or behaviours (Arac et al., 2019; Inayat et al., 2020) or both. *AutoGaitA* is thus unique in that it is specifically developed for post-hoc (i.e., following posture tracking) kinematic analyses that are independent of the species and behaviour under study. *AutoGaitA* also standardises kinematic analyses across labs, is not limited to a few kinematic features and allows cross-species comparisons.

Appendix - Detailed User Workflows

Graphical User Interfaces and Installation

AutoGaitA's central goal is to provide a user-friendly experience, allowing scientists to focus on their research questions instead of spending unnecessary hours manually computing features and statistical tests or visualising results. For this purpose, we provide three graphical user interfaces (GUIs) designed to keep the amount of necessary information and configuration to a minimum while providing sufficient flexibility for users to tailor *AutoGaitA's* analyses to their needs. **Figure A.1** depicts the main menus of *AutoGaitA_DLC* (**Figure A.1A**), *AutoGaitA_Simi* (**Figure A.1B**), and *AutoGaitA_Group* (**Figure A.1C**). Nonetheless, *AutoGaitA's* full capabilities can be accessed also via the command line (see online documentation).

A. DLC

B. Simi

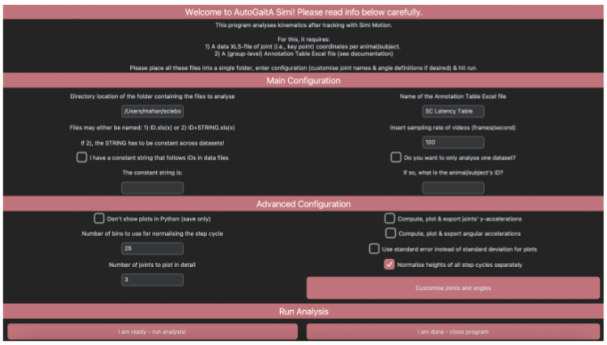

C. Group

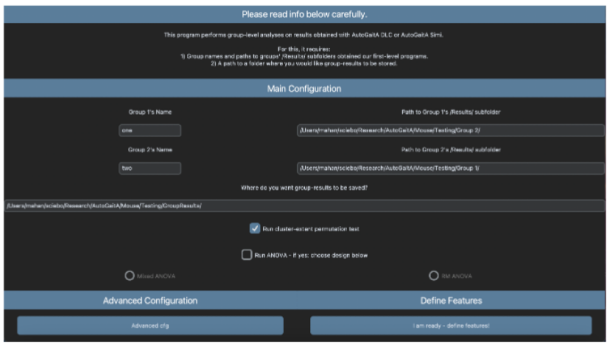

Figure A.1. AutoGaitA's graphical user interfaces (GUIs). *First-level analyses (**A,B**) follow the workflow of **Figure 1**. Group analyses (**C**) are performed on the results of the first-level analyses. All analyses and configuration parameters can also be assessed via the command line.*

AutoGaitA is being released alongside this paper as an open-source beta version and its code, readme, documentation, and tutorials are available on the *AutoGaitA* GitHub repository (https://github.com/mahan-hosseini/AutoGaitA). We stress the importance of keeping *AutoGaitA* updated since new features and bug fixes will be provided regularly. We rely on users to report bugs and assist with *AutoGaitA's* development. Bugs and feedback can be provided to autogaita@fz-juelich.de, and is highly appreciated.

Preparation of Annotation Tables

The *Annotation Tables* (Excel files) inform *AutoGaitA* about the timestamps (in seconds with two decimal precision, e.g., 1.22s) of individual occurrences of the behaviour of interest in a given input video. For locomotion, the behaviour of interest is a step cycle, defined as the time window from the onset of a swing phase until the offset of the following stance phase. *AutoGaitA* reads the time information provided in the *Annotation Tables* and uses this information for its plots and to normalise and average, for example, step cycles. *Annotation Tables* offer a lot of flexibility. Users can, for example, keep the same input dataset folder containing all their videos and tailor the *Annotation Table* to only include, e.g., steps before slips, steps made immediately before turning, or anything else that might be of research interest to generate *Results* folders that correspond to different analyses.

Users are strongly encouraged to follow the following procedure. First, users should carefully read the instructions provided in the *Preparation* section of our documentation. Subsequently, users are asked to download the (DLC or Simi) template and example files (respective links are provided in our repository as well as in the *Downloads* subsections of the *Annotation Table sections* of our documentation) and 1) use the template file to enter their data's timestamp information and 2) use the example file to confirm that their resulting *Annotation Table* looks

similar. This procedure is also explained in a tutorial video on our YouTube channel (https://youtube.com/@autogaita).

Extracts from example *Annotation Tables* are provided in **Figure A.2** for DLC and Simi, respectively. The first couple of columns inform *AutoGaitA* about the video to which the timestamps that follow in later columns correspond to.

A. DLC

ID	Genotype	Run	SC Number	Swing (ti)	Swing (te)	Stance (te)	Swing (ti)	Swing (te)	Stance (te)
10	PCCD3	1	3	1,72	1,87	2,03	2,04	2,12	2,38
		2	3	1,09	1,23	1,39	1,97	2,15	2,35
		3	3	1,51	1,64	1,91	1,92	2,02	2,39
11	PCCD3	1	3	1,81	1,94	2,38	3,62	3,75	3,95
		2	2	1,25	1,39	1,52	1,53	1,66	1,77
		3	3	4,92	5,02	5,32	5,33	5,4	5,56
12	PCCD3	1	0						
		2	3	1,66	1,84	2,03	2,04	2,2	2,49
		3	2	5,49	5,65	5,96	7,48	7,62	7,93

B. Simi

ID	Condition	Leg	Run	SC Number	Swing (ti)	Swing (te)	Stance (te)	Swing (ti)	Swing (te)	Stance (te)
Y_07	young									
		left	1	2	3,88	4,28	5	5,01	5,39	6,11
			2	2	8,43	8,84	9,55	9,56	9,97	10,76
			3	2	12,26	12,66	13,38	13,39	13,78	14,54
		right	1	3	3,35	3,69	4,44	4,45	4,84	4,56
			2	2	7,89	8,26	9	9,01	9,4	10,14
			3	2	12,83	13,23	13,96	13,97	14,34	15,14

Figure A.2. Example entries in Annotation Tables. A) *Depicting an example for the DLC and mouse timestamp annotation and* ***B)*** *example for the Simi and human timestamp annotation. The first columns inform AutoGaitA about which video the last columns' time information refers to, i.e. the animal/subject ID, the genotype/condition, the trial number (in this case, the run number), and how often the behaviour of interest was seen in the trial (step cycle (SC) Number). Swing (ti) and Stance (te) columns define a step cycle's start and end times for the study of locomotion but can be used for any other behaviour that the user might be interested in. Studying an individual type of step in the same dataset (e.g. only considering steps before slips, or only steps with a stride of 200 msec)) can be achieved solely via modifying the values entered in the Annotation Tables, without the necessity to modify the input datasets themselves in any way. For detailed instructions, templates, as well as example files see our YouTube channel, repository and documentation.*

AutoGaitA_DLC: From Videos (of mouse locomotion) to Plots

Users are advised to watch the tutorial videos we provide on our YouTube channel (https://youtube.com/@autogaita).

File Naming

To ensure standardisation across laboratories, we started by generating a file naming convention (*see also online documentation*). The recorded video files should be named with the following structure, *[A]_[B]_[C]_[D]-[E]*, with *[A]* being a unique prefix to identify the animal group used for the experiment (e.g. C57B6 for C57BL6/J mice or WT for wild-type animals), *[B]* the number uniquely identifying an individual animal in each group, *[C]* the motor task executed, *[D]* trial number, *[E]*, the camera identifier if videos are acquired from multiple sources. For example, the video recorded from camera 6 (*E)* of the first trial (*D)* of a C57BL6/J (*A)* Mouse number (*B)* 10 walking on a 25 mm wide beam (*C)* will be saved as *C57B6_Mouse10_25mm_Run1-6DLC*. Following tracking with DLC, DLC-dependent suffixes are added to the file name, *[A]_[B]_[C]_[D]-[E][G]*, with *[G]* indicating the type of tracking done. For example, if the experimenter tracked both the mouse and the beam, *[G]* will make a specific reference to one of the two .CSV files with the tracked coordinates. In the example above the names of the DLC-generated files will be: *C57B6_Mouse10_25mm_Run1-6DLC-JointTracking* for the labelling of joint coordinates and *C57B6_Mouse10_25mm_Run1-6DLC-BeamTracking* for the labelling of the beam coordinates. This naming convention allows a high degree of flexibility in the usage of our toolbox, as it ensures that *AutoGaitA* can extract the important information from the file names across multiple tasks, species, or genotypes.

Locomotion cycle annotation

After ensuring that naming convention rules are followed, experimenters need to manually annotate the stance and swing phases of the individual step cycles they want to analyse within each video, e.g. excluding footslips or selecting only the steps before a footslip. The step cycle

timestamps should be entered into the Annotation Table, as described above (see **Figure A.2**) and in detail in the documentation and stored in the same directory in which the DLC files are located.

Main Configurations

Once these preparatory steps are completed, *AutoGaitA_DLC* can load and analyse individual videos or batches. The *Main Configuration* panel of the GUI asks to insert information to analyse the dataset: a) the frame/second rate at which the videos were acquired (obligatory field), b) convert pixel to mm (optional field), c) invert the y-axis coordinates (optional field), d) normalise the y-coordinates to a baseline reference, such as floor or beam (optional field), e) adjust the x-coordinates to follow the motion direction, important to compare results if animals walk both from left-to-right and from right-to-left (optional field).

Advanced Configurations

Additional settings can be customised by clicking the "*Advanced configuration*" button. This window allows users to a) customise the name and numbers of joints tracked to match the names used in the DLC tracking, and to define how (i.e., using which 3 joints/angle) angles are calculated (note that, being developed with mouse data, hindlimb joints default to hindpaw, ankle, knee, hip, and iliac crest, and angles to ankle, knee, and hip), b) edit the parameters used for the analysis, c) define additional output settings. Using the advanced settings, users can set the values of the x- and y-coordinates that, if exceeded, will make *AutoGaitA* discard that step cycle. This is important to account for eventual inaccuracies in the tracking, with joints being labelled outside the area occupied by the mouse in the video. Next, they can decide the number of bins that the normalised step cycle is divided into. Each step cycle is normalised to 100%, with the default setting dividing the data points into 25 bins, with each data point representing 4% of the full locomotion cycle. Users can represent the data at a higher (increase bin number) or lower (decrease bin number)

resolution. Users can also decide whether the acceleration of joints (along the horizontal axis) and angles should be included in the analysis. Height values are, by default, normalised across the whole dataset. That is, *AutoGaitA* finds the lowest height value across the entire body and the full dataset and sets all heights so that this (across-body and throughout-time, henceforth called *global*) minimum is set to zero. For example, if the global height minimum should be -0.2, *AutoGaitA* adds 0.2 to all height values across the dataset. If users expect their cameras to introduce distortions or know that their floor is uneven, it is recommended to perform this height-normalisation step *for each step cycle anew*. We provide a checkbox to choose whether this should be done in the advanced configuration window. However, users should consider that performing the height normalisation at the step level will mean that output Excel files' height values no longer correspond to those present in the input data.

Customise AutoGaitA's Output

Finally, the output can also be tuned to user preferences. Users can choose how many (hind limb) joints to plot in detail. For example, users can choose to analyse 10 joints of their interest. *AutoGaitA* will compute the velocities and (if wanted) accelerations of all 10 joints and include these values in the output .XLS files as well as in figures that plot features (e.g., joints' heights) over the *average step cycle*. In addition to this, users can choose to plot the first, for example, 4 joints in detail. This means that a) a stick diagram using these four joints and b) additional plots of joint height for each *individual step cycle* will be generated. Users can further decide whether the error bars should represent standard errors instead of standard deviations and whether output sheet files should be stored as .XLSX instead of .CSV.

Data Input

Once all settings are chosen (which will remain unchanged after a run has been executed as long as the GUI is not closed), analysis can run on a single video or batches of videos. Selecting the option "One Video" will open the *SingleGaitA* window, in which the user must define certain information so that the algorithm can correctly read and analyse the coordinates. First, users need to insert the directory of the folder containing the files for analysis and the file name of the Annotation Table. Next, to select the correct and corresponding body (and beam) coordinate and video files for the analysis, users need to specify information about their file names. This ensures *AutoGaitA*'s versatility, allowing analyses of diverse species and tasks. The user must define the "unique subject identifier" (*[B]* in the file naming convention), i.e., what precedes the number of the subject. In our convention of *[A]_[B]_[C]_[D]-[E][G]* and our example of *C57B6_Mouse10_25mm_Run1-6DLC-JointTracking*, the unique subject identifier would be "Mouse". This identifier is important to load data from any species, e.g. mouse, flies, worm data. Next, as multiple rhythmic behaviours can be analysed, the "unique task identifier" (*[C]*), e.g. beam, ladder, treadmill, must be provided. In the example above, the unique task identifier is "_25mm". Please note that the underscore "_" has to be provided in this case. Next, the "unique trial identifier" (*[D]*), e.g. run, trial, or pull, must be defined, being "Run" in our case. Finally, as multiple cameras can be used to record behaviour, users must insert the "unique camera identifier" (*[E]*), being "-6DLC" in our case (please be sure to provide the hyphen "-" for these). To clarify, the algorithm needs to know what *exactly* is written immediately before and after the ID (here mouse) number (*[B]* & *[C]*, respectively, thus requiring the underscore "_" to be provided in *[C]*) and before and after the trial number (*[D]* & *[E]*, respectively, thus requiring the hyphen "-" to be provided in *[E]*). Users finally must insert the unique identifier for the DLC-added suffix (*[G]*) to

load the .CSV file containing the joint coordinates and, if existing, the .CSV file containing the tracked beam or baseline for y-coordinates. In our example above, that would correspond to "JointTracking". Users should pay attention to all identifiers being unique, meaning appearing exactly once in file names.

Results Output

At this point, *AutoGaitA* runs the analysis and generates a *Results* folder with separate subfolders for each video analysed. An example *Results* subfolder (of one of the example datasets (*Mouse 18, Run 2, 25mm*) we provide in the *AutoGaitA* repository's *example data* folder) is shown in **Figure A.3A** (note that this folder can include many more figures if users decide to analyse more joints/angles and features). Each subfolder includes the original DLC-tracked data files and videos of joint coordinates and, if included, the baseline height tracking. Furthermore, each subfolder contains four Excel (or *csv*) files. The Excel files provide all (original DLC-provided and new *AutoGaitA*-computed) features of original and normalised step cycles as well as after computing features' averages and standard deviations across step cycles. An extract of an *Average Stepcycle.xlsx* file is shown in **Figure A.3B**, presenting the numerical values of the first four features after averaging the three step cycles of this run. Note that the *SC Percentage* column implements increments of 4% percentiles since step cycles were normalised to the default value of 25 bins. *AutoGaitA* further generates various figures visualising features for single and averaged step cycles in *.png* and *.svg* format. We provide the stick diagram of the hindlimb and the ankle angle over time as examples of figures plotted over single step cycles (in this case three) in **Figure A.3C** and **A.3D**, respectively. **Figures A.3E** and **A.3F** illustrate step cycle averages of joint angles and accelerations, respectively. *AutoGaitA* also generates a text file indicating if any issues were encountered during the analysis (see *Issues.txt* in **Figure A.3A**). The information stored in this text

file corresponds to what is displayed in the command window while *AutoGaitA* is performing the analysis.

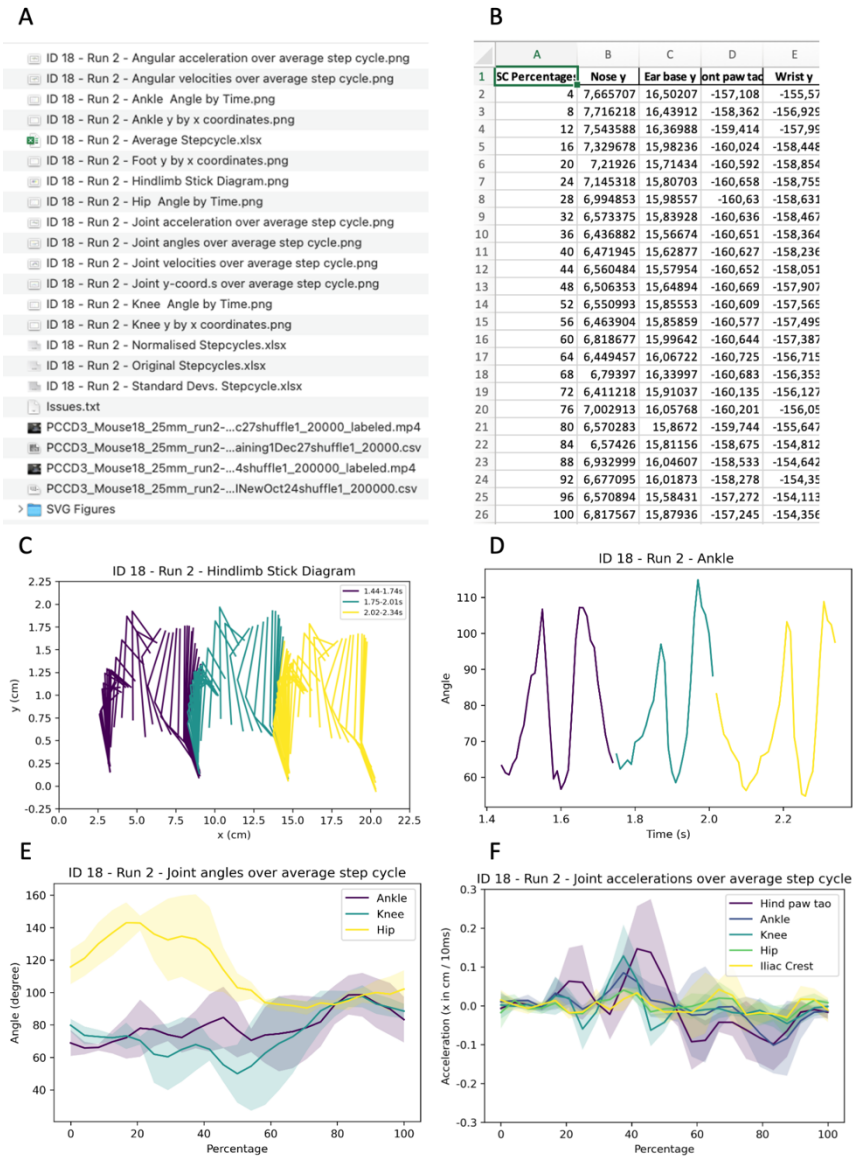

Figure A.3. AutoGaitA_DLC's Example Results. A) *Example subfolder for Mouse 18, Run 2 (provided in the example datasets subfolder of our repository).* ***B)*** *Extract from Average Stepcycle.xlsx file illustrating numerical values of the first four features over the average of the three step cycles of this run.* ***C,D)*** *Example figures illustrating single step cycles, plotting the hindlimb stick diagram* ***(C)*** *and the ankle angle* ***(D). E,F)*** *Example figures illustrating the average step cycle, plotting joint angles* ***(E)*** *and accelerations* ***(F)****.*

AutoGaitA_Simi: From Videos (of human locomotion) to Plots

Users are advised to watch the tutorial videos we provide on our YouTube channel (https://youtube.com/@autogaita).

Locomotion cycle annotation

After recording the videos of human locomotion, experimenters need to manually annotate the stance and swing phases of the individual step cycles, which they want to analyse within each video, as described in the methods section below regarding the (pre-)processing of human gait data. The annotated step-cycle timestamps should be entered in an *Annotation Table*, as described in detail in the *Preparation of Annotation Table* section of this appendix. Users need to ensure that subject IDs match between the *Annotation Table* and input data files. The *Annotation Table* must be stored in the same folder as the data files.

Main configurations

Once these preparatory steps are completed, *AutoGaitA_Simi* can load and analyse individual datasets or multiple datasets at once (i.e., batches). The main (i.e., standard) configuration panel of *AutoGaitA*'s GUI requires the following information to analyse the dataset: a) the directory to the folder containing the data files (obligatory field) and b) in case a constant string is appended to the IDs, the label of the constant string (optional field). This constant string is important since it allows experimenters to store information about their experimental groups in filenames (e.g., Subject7_Patient and Subject7_Control). It further prevents *AutoGaitA* from being confused if other, unrelated Excel files should be stored in the directory (note that the algorithm, if analysing in batch, will attempt to analyse any Excel file present in the folder if no constant string is appended to file names). Users have to further provide c) the name of the Annotation Table (obligatory field), d) the frame/second rate at which the videos were acquired in Hertz (obligatory field), and e), in case the user only wants to analyse a single dataset, the ID of the dataset of interest (optional field).

Advanced configurations

Due to the variability in step length within an individual, step cycles need to be normalised. Using the advanced configuration panel of *AutoGaitA*'s GUI, users can decide the number of bins the normalised step cycle is divided into. Each step cycle is normalised to 100%, with the default setting dividing the data points into 25 bins, with each bin representing 4% of the full cycle. Users can represent the data at a higher (increase bin number) or lower (decrease bin number) resolution. Users can also decide whether to compute and plot the acceleration of joints and angles in the analysis. Height values are, by default, normalised across the whole dataset. That is, *AutoGaitA* finds the lowest height value of the body and across the full dataset and sets all heights so that this (across-body and throughout-time, henceforth called *global*) minimum is set to zero. For example, if the global height minimum should be -0.2, *AutoGaitA* adds 0.2 to all height values across the dataset. If users expect their cameras to introduce distortions or know that their floor is uneven, it is recommended to perform this height-normalisation step *for each step cycle anew*. We provide a checkbox to choose whether this should be done in the advanced configuration window. However, users should consider that, due to the manipulation of the height ratios across step cycles, output Excel files' height values do not correspond to those present in the input data (i.e., the heights observed in the videos) any longer.

Customise AutoGaitA's Output

*AutoGaitA'*s output can also be tuned to user preferences. Users can choose how many joints to plot in detail. For example, using the *Custom column names & features* window of the advanced configuration, users can choose to analyse 10 joints of their interest. *AutoGaitA* will compute the velocities and (if wanted) accelerations of all 10 joints and include these values in the output .XLS files as well as in figures that plot features (e.g., joints' heights) over the *average step cycle*. In

addition to this, users can choose to, for example, plot the first 4 joints in detail. This means that a) a stick diagram using these four joints and b) additional plots of joint-height for each *individual step cycle* will be generated. Users can further choose error bars to represent standard errors instead of standard deviations. Apart from specifying the number of joints and angles to be analysed, the *Configure custom column names & features* menu enables any species to be analysed, allowing users to customise the name and numbers of joints tracked to match the names used in the Simi tracking, and to define how (i.e., using which three joints) each angle of interest should be calculated.

Results output

Once settings are configured according to user needs, the analysis can be run. At this point, *AutoGaitA* generates a *Results* folder with separate subfolders for each video analysed. An example *Results* subfolder is shown in **Figure A.4A** (note that this folder can include more figures if users decide to analyse more joints/angles and features). Each subfolder includes the original Simi-tracked data files of joint coordinates. Furthermore, each subfolder contains four Excel files that include the numerical values of: (i) all features of the original step cycles, (ii) all features of the normalised step cycles, (iii) feature averages and (iv) feature standard deviations. Averages and standard deviations are computed at the step cycle-level and for each subject separately. An extract of an *Average Stepcycle.xlsx* file is shown in **Figure A.4B**, presenting the numerical values of the first four features after averaging the 17 step cycles the left leg performed in this run. Note that all four Excel files contain three sheets each, including features of steps performed by the left, the right, or across both legs. Note that the *SC Percentage* column implements increments of 4% percentiles since step cycles were normalised to the default value of 25 bins. *AutoGaitA* further generates various figures visualising features for single and averaged step cycles in *.png* and *.svg*

format. We provide the stick diagram of the left leg and its ankle angle over time as examples of figures plotting single step cycles (in this case 17) in **Figure A.4C** and **A.4D**, respectively. **Figures A.4E** and **A.4F** illustrate step cycle average figures, plotting joint angles and accelerations of the left leg, respectively. *AutoGaitA* also generates a text file indicating if any issues were encountered during the analysis. The information stored in this text file corresponds to what is printed to the command window while *AutoGaitA* is performing the analysis.

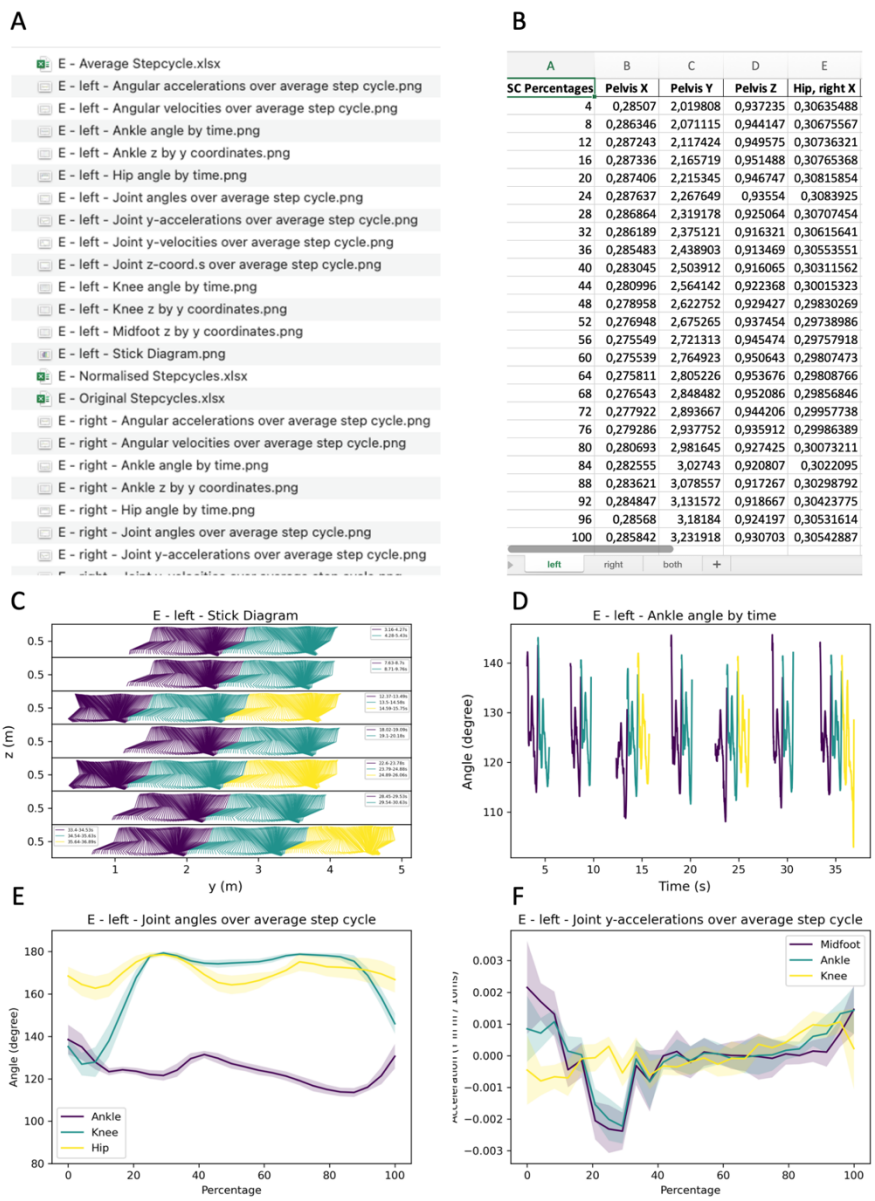

SC Percentages	Pelvis X	Pelvis Y	Pelvis Z	Hip, right X
4	0,28507	2,019808	0,937235	0,30635488
8	0,286346	2,071115	0,944147	0,30675567
12	0,287243	2,117424	0,949575	0,30736321
16	0,287336	2,165719	0,951488	0,30765368
20	0,287406	2,215345	0,946747	0,30815854
24	0,287637	2,267649	0,93554	0,3083925
28	0,286864	2,319178	0,925064	0,30707454
32	0,286189	2,375121	0,916321	0,30615641
36	0,285483	2,438903	0,913469	0,30553551
40	0,283045	2,503912	0,916065	0,30311562
44	0,280996	2,564142	0,922368	0,30015323
48	0,278958	2,622752	0,929427	0,29830269
52	0,276948	2,675265	0,937454	0,29738986
56	0,275549	2,721313	0,945474	0,29757918
60	0,275539	2,764923	0,950643	0,29807473
64	0,275811	2,805226	0,953676	0,29808766
68	0,276543	2,848482	0,952086	0,29856846
72	0,277922	2,893667	0,944206	0,29957738
76	0,279286	2,937752	0,935912	0,29986389
80	0,280693	2,981645	0,927425	0,30073211
84	0,282555	3,02743	0,920807	0,3022095
88	0,283621	3,078557	0,917267	0,30298792
92	0,284847	3,131572	0,918667	0,30423775
96	0,28568	3,18184	0,924197	0,30531614
100	0,285842	3,231918	0,930703	0,30542887

Figure A.4. AutoGaitA_Simi's Example Results. A) *Example subfolder for Subject E.* ***B)*** *Extract from the Average Stepcycle.xlsx file illustrating numerical values of the first four features over the average of the 17 step cycles of this run. Note that all Excel files contain three sheets showing values of steps performed by the left, right, or across both legs.* ***C,D)*** *Example figures illustrating single step cycles, plotting the left leg's stick diagram* ***(C)*** *and the ankle angle* ***(D). E,F)*** *Example figures illustrating the average step cycle of the left leg, plotting joint angles* ***(E)*** *and accelerations* ***(F)****.*

AutoGaitA_Group

Users are advised to watch the tutorial videos we provide on our YouTube channel (https://youtube.com/@autogaita).

Main Configuration

While *AutoGaitA's* first-level tools (*AutoGaitA_DLC* and *AutoGaitA_Simi*) analyse single datasets, *AutoGaitA_Group* is able to compare up to 6 groups with each other. *AutoGaitA_Group* reads the *Results* folders created by the first-level tools and requires that each group's *Results* folder only contains the results of that group (i.e., results of distinct groups should never be combined in a folder manually). The main configuration window only requires users to enter groups' names and the locations of their corresponding *Results* folders as well as the directory to which group results should be stored. It is important to highlight that the (user defined) configuration of first-level analyses must match between groups.

Advanced Configurations

For statistical analysis, *AutoGaitA* provides a cluster-extent permutation test, which is recommended for comparing the entered data. However, additional two-way analyses of variance (ANOVAs) corrected with Tukey's method can be performed. Under the *advanced cfg settings,* the number of permutations of the cluster-extent test can be set (at least 10.000 is recommended), as well as the alpha level of statistical significance, and if figures plotting averages should adopt standard deviations or standard errors as error bars. Users can set how many principal components shall be computed in *AutoGaitA_Group's* PCA analysis and whether its 3D scatterplot should also be exported as a video file (**Figure A.5** and **Supplemental Video S4**).

Define features and run analysis

Once the configuration is set, users must choose which features to test statistically and which to include in the PCA analysis. For that, *AutoGaitA_Group* automatically detects the features of the first-level analyses and lists them in a separate window. If the first-level analysis was performed with *AutoGaitA_Simi*, users must additionally choose which body-side should be compared.

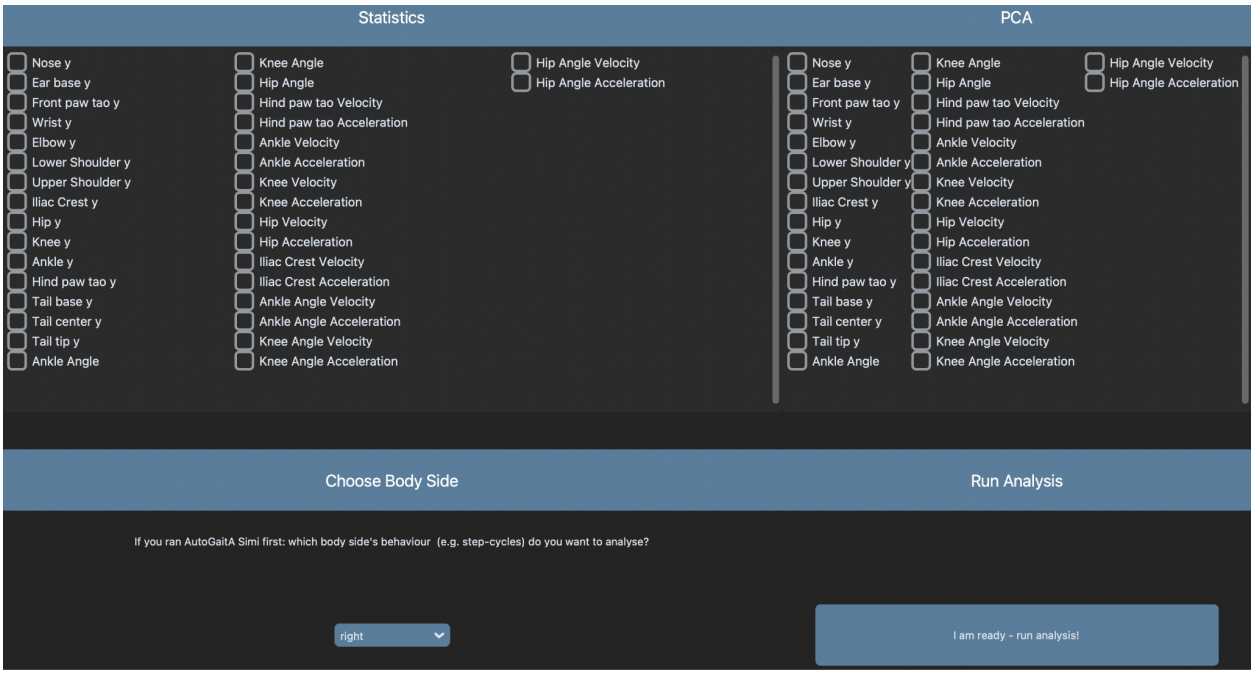

Figure A.5. *AutoGaitA_Group's* Features Window. After configuring the location of the *Results* folders, group names, and advanced options, users determine which features to test statistically and assess with PCA in this window. If *AutoGaitA_Simi* was performed at the first level, users must additionally configure which body side the behaviour should correspond to (e.g., steps performed by the left leg).

Results Output

At this point, the analysis can be run. Users can overview the progress in the command line. Depending on the amount of data, the number of features, and the number of permutations, this process may take a while. At this time, *AutoGaitA* generates a *Group Results* folder at the location the user configured. An example *Group Results* folder of the mouse beam width (5 mm, 12 mm, 25 mm) analysis presented in Showcase 1 is shown in **Figure A.6A**. *AutoGaitA_Group* generates

six Excel files per group, providing the numerical values of features for each group's original and normalised step cycles, standard deviations, and averages across subject- or group-level step cycles. An extract of a *Grand Average Group Stepcycles.xlsx* file is provided in **Figure A.6B**, showing the first five columns for that group's overall average (i.e., averaging first all steps for each subject and then averaging those averages across subjects). *N, SC Percentage* and *SC Number* columns inform about the group's sample size, the percentiles of the average step cycle (4% percentiles for our default value of 25 bins for normalisation) and the average number of step cycles performed by a subject.

Further, group-level figures are provided which illustrate a given set of *different features* (e.g., accelerations, velocities, heights, or angles) for the hindlimb *for the same group*. **Figure A.6C** shows an example, plotting the three hindlimb angles over the average step cycle for mice that walked over the narrow (5mm) beam. Naturally, across-group comparisons are oftentimes more interesting. *AutoGaitA_Group* therefore provides, for all features of interest, figures plotting the *same feature across different groups* over the average step cycle, too. Figure YD shows an example, plotting the average angle of the ankle for the three beam width groups introduced earlier. Note that *AutoGaitA_Group* generates these figures for all features that were configured in first-level tools as (hindlimb) joints and angles (see the *Custom column names and features* section of our documentation).

Further, *AutoGaitA_Group* provides the results of the statistical analyses in figures as well as exact numerical results (e.g., values of p-values) in a *Stats.txt* file. **Figures A.6E** and **A.6F** show example figures after applying the cluster-extent permutation test and Tukey's multiple comparisons for testing the three pairwise comparisons of our beam width perturbation for differences in the angle of the ankle. Finally, PCA results are provided in 2D and 3D scatterplot

figures (**Figures A.6G** and **A.6H**), an optional 3D scatterplot video (**Supplemental Video S4**), and an *PCA Info* Excel file providing the exact numerical values for the percentage of explained variance of each principal component and eigenvectors of each feature / principal component combination. Note, all figures are again provided as *.png* as well as *.svg* files.

A

- 5 mm - Angular velocities over average step cycle.png
- 5 mm - Average Group Stepcycles.xlsx
- 5 mm - Grand Average Group Stepcycles.xlsx
- 5 mm - Grand Standard Deviation Group Stepcycles.xlsx
- 12 mm - Joint angles over average step cycle.png
- 12 mm - Joint velocities over average step cycle.png
- 12 mm - Joint y-coord.s over average step cycle.png
- Knee - angle over average step cycle.png
- Knee - Velocities over average step cycle.png
- Knee - Y-coord.s over average step cycle.png
- Knee Angle - Cluster-extent Test.png
- Knee Angle - Tukey's Multiple Comparison Test.png
- Knee y - Cluster-extent Test.png
- Knee y - Tukey's Multiple Comparison Test.png
- Knee- Angular Velocities over average step cycle.png
- PCA 3D Scatterplot.mp4
- PCA 3D Scatterplot.png
- PCA Info.xlsx
- PCA Scatterplot.png
- Stats.txt
- SVG Figures

B

A	B	C	D	E
N	SC Percentage	SC Number	Nose y	Ear base y
20	4	6,85	4,619785	13,88416
20	8	6,85	4,656197	13,70255
20	12	6,85	4,825829	13,47314
20	16	6,85	4,816759	13,42181
20	20	6,85	4,664362	13,36743
20	24	6,85	4,881739	13,56716
20	28	6,85	5,437106	14,02817
20	32	6,85	5,409923	13,88196
20	36	6,85	5,846483	13,7989
20	40	6,85	5,713814	13,93155
20	44	6,85	5,94764	13,79988
20	48	6,85	5,811998	13,89055
20	52	6,85	5,736118	14,56336
20	56	6,85	6,418038	13,79258
20	60	6,85	5,936583	14,18836
20	64	6,85	6,053372	14,06756
20	68	6,85	5,791334	13,8393
20	72	6,85	7,141268	14,20763
20	76	6,85	6,41803	13,82677
20	80	6,85	7,732641	14,2761
20	84	6,85	8,559941	13,70631
20	88	6,85	8,554806	13,87863
20	92	6,85	6,71112	13,86893
20	96	6,85	8,560472	13,84245
20	100	6,85	9,048777	13,4771

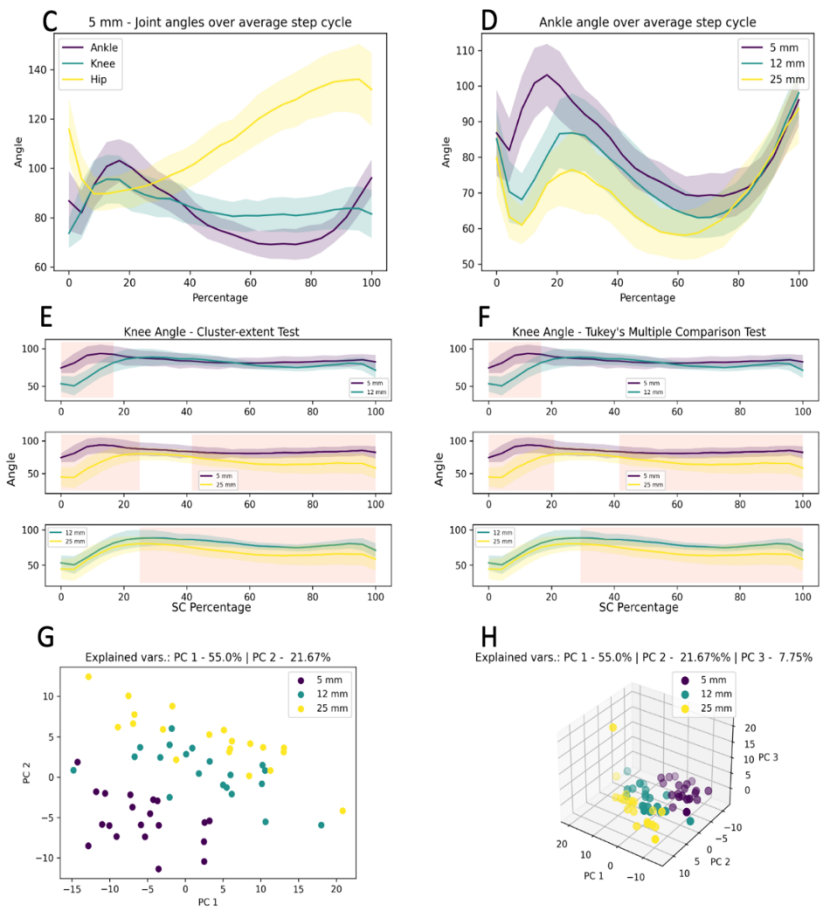

Figure A.6. AutoGaitA_Group's Example Results. *A) Example Group Results folder.* ***B)*** *Extract from Grand Average Stepcycle.xlsx file illustrating numerical values of the first three features over the average step cycles of a group.* ***C)*** *Example figure showing different features (here, angles) of the same group.* ***D)*** *Example figure showing the same feature (here, ankle angle) for different groups.* ***E, F)*** *Figures displaying the results of the statistical procedures. Results were obtained after performing the cluster-extent permutation test* ***(E)*** *and Tukey's multiple comparison test* ***(F)*** *for all three pairwise contrasts.* ***G, H)*** *Results of PCA. Results were obtained after reducing features to a two-* ***(G)*** *or three-* ***(H)*** *dimensional principal components space.*

Methods

AutoGaitA_Group's Statistical Procedures

AutoGaitA_Group provides two approaches for the statistical assessment of features across groups, a cluster-extent permutation test and an ANOVA approach. The cluster-extent permutation test is strongly recommended over the ANOVAs due to its lack of parametric assumptions. Nonetheless, we provide the ANOVA approach in the toolbox, and present ANOVA results when showing our own empirical findings in this paper, since it is the most prominent test adopted in the field of motor control.

Cluster-extent permutation test

AutoGaitA's cluster-extent permutation test follows the concepts introduced by Maris and Oostenveld (2007). For a given feature of interest, two groups will be compared to each other at each given time bin with independent-sample t-tests, obtaining, with the default setting of normalising step cycles to 25 bins, 25 p-values. If a given p-value is smaller than 0.05, it is marked as significant at the first-level. Data points with significant (first-level) p-values after their corresponding t-test form clusters. Cluster size is then defined as the sum of all t-values in a given cluster. If the t-test was not significant, cluster size is set to 0. If a single data point was significant and temporally adjacent data points were not significant, cluster size is equal to that data point's t-value. If two data points that are temporally adjacent to the significant data point both had significant p-values, cluster size is set to the sum of the corresponding 3 t-values, etc. This provides true observed cluster sizes that will be tested against maximal cluster sizes under the null hypothesis next.

For the permutation procedure group labels are randomly shuffled (called "null data" henceforth to indicate that possible effects between groups have been removed). The same

procedure of 25 t-tests as described above is performed on the null data, which provides 25 values of cluster sizes under the null hypothesis. The largest cluster size is extracted and stored in a distribution. This procedure is repeated 10.000 times (recommended). This results in 10.000 values of maximal cluster sizes under the null. The true observed cluster sizes are tested against this distribution of maximal cluster sizes under the null, computing p-values of a true observed cluster as the proportion of maximal clusters under the null equal to or larger than that true observed cluster.

If users want to compare more than two groups in their analysis, the same concept applies. However, the first-level and the permutation procedures of t-testing and recording cluster size are performed for all pairwise comparisons in sequence. For example, if users test three groups, the first-level analysis of 25 t-tests is performed three times, once for each pairwise comparison. True observed cluster sizes are stored as explained above. For the permutations, group labels are shuffled conserving the original data's sample size distributions across groups, and the procedure of first-level t-tests is repeated 10.000 times on the null data. This again provides 10.000 maximal cluster sizes under the null that is used for testing true observed cluster sizes. Critically, for each of the 10.000 permutations, the biggest cluster size now is obtained *across all three pairwise comparisons*! For example, if, under the null, testing group A vs. B would yield a biggest cluster size with a t-value sum of 33 and the comparison B vs. C would yield a biggest cluster with a t-value sum of 39, we would store 39 for this permutation. Storing the maximal cluster size across all three contrasts in this manner is an example of permutation procedures automatically correcting the family-wise error rate as long as the exact same procedure for obtaining true observed and permuted (i.e., null data) cluster sizes (or any test statistic of interest for that matter) is adopted.

A simulation analysis was performed to assess the validity of the cluster-extent permutation test in this context. For that, a sample of 38 human subjects that was analysed with *AutoGaitA_Simi* was used. Importantly, for these simulations, the 38 subjects were randomly assigned into two groups of 19 subjects each. The permutation test was applied to the height value (i.e., Z coordinate) of the right midfoot. This procedure was repeated 10.000 times and a distribution of cluster-level p-values was generated. The rationale of this approach is that a valid statistical test yields an approximately uniform distribution of p-values in the absence of an effect in the dataset (*under the null*). Setting the alpha level of statistical significance, it was particularly important to demonstrate that our test does not generate significant results more often than 5% under the null as this would imply a biased procedure and an unacceptably high risk of a Type 1 error. **Figure A.7** presents the distribution of cluster-level p-values that were smaller than 1, which is approximately uniform. We discarded cluster p-values of 1 in this analysis since these correspond to a non-significant first-level result (i.e., no cluster being formed). The main metric that should be focussed on is the proportion of cluster-level p-values smaller than 0.05 with respect to cluster-level p-values smaller than 1. This metric assesses the Type I error rate, i.e., *given that a cluster was formed ($p<1$), how often was the null-hypothesis rejected ($p<0.05$) in the absence of an effect in the datasets?* This value was 0.042 for the cluster-extent test, suggesting its validity.

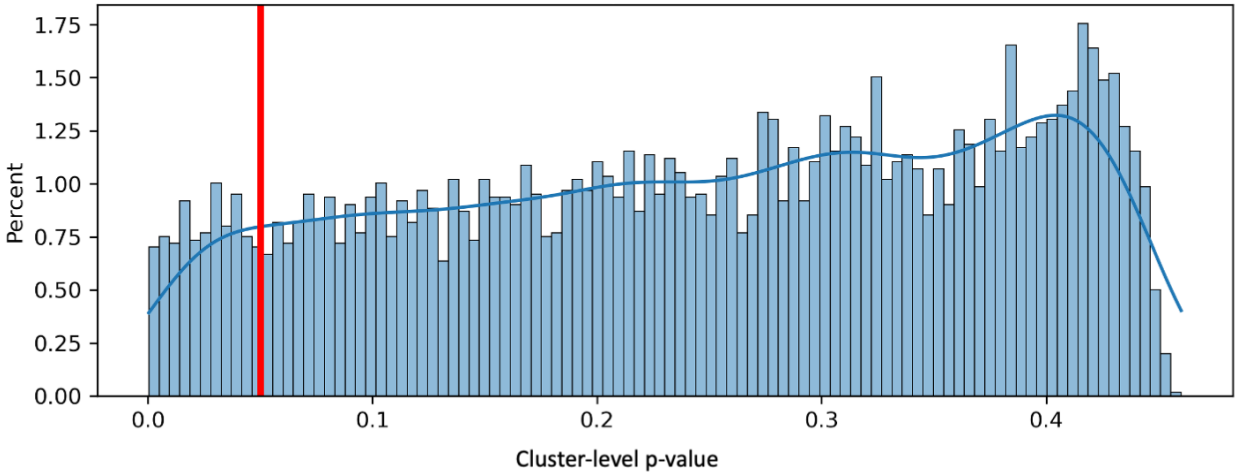

Figure A.7. Testing the validity of the cluster-extent permutation test. *Distribution of cluster-level p-values smaller than 1 after applying the cluster-extent permutation test 10000 times on randomly shuffled (i.e., null) human data of midfoot z (i.e., height) coordinates. This distribution should be approximately uniform and, given a significant first-level test (i.e., a cluster was formed), generate p-values smaller than 0.05 (indicated by the red vertical line) at most 5% of times. Our test generated such p-values 4.2% of times, suggesting its validity.*

Two-way ANOVAs corrected with Tukey's method

Users can opt to perform two-way ANOVAs to obtain clusters of pairwise differences in their features of interest. For that, it is critical to inform our toolbox whether the experimental design is fully repeated (i.e., each group consists of the same individuals), such as in our case of the same group of mice walking over beams of different widths, or mixed (i.e., each group consists of different individuals), as in our case of contrasting young and old humans. *AutoGaitA* automatically checks the assumption of sphericity for the main effect of step cycle percentage and corrects its p-value if sphericity is not met using the Greenhouse-Geisser correction. Given that the main effect of step cycle percentage was significant we perform pairwise tests at all step cycle percentiles correcting for multiple comparisons using Tukey's honestly significant difference.

Experimental mouse model

Mice were maintained following the protocols for animal experiments approved by the local health authority in North Rhein Westphalia (LANUV, Landesamt für Natur, Umwelt und

Verbraucherschutz Nordrhein-Westfalen). 3 month-, 9-month and 24-month-old C56BL6/J mice of both sexes were used for behavioural experiments. Analysis of the behavioural data showed similar responses in male and female mice. Mice had *ad libitum* access to food and water, and were housed in groups of maximum 5 animals, maintained on a 12-hour dark/light cycle within a room controlled for humidity and temperature.

Motor behaviour test

To assess motor coordination and its age-dependent adaptation, mice of different ages were tested as they crossed 1.3-meter-long beams with different widths (5 mm, 12 mm, and 25 mm). On the first day, mice were tasked to cross the wide beam 25 mm, second day the 12 mm one, and third day the 5 mm one. For each beam size three to five trials per mouse were recorded using eight high-speed cameras (mV Blue Cougar XD; 100 frames/second) positioned around the beam (3D Simi Motion). Multiple camera views were analysed to count the number of slips, which were then averaged across trials per individual mouse.

2-D kinematic reconstructions

To reconstruct the 2D kinematics of hindlimb and forelimb coordination across ages and beams, we used the videos captured by the camera placed perpendicularly to the beam. Markerless mice walking in both directions were captured, so our data are averages of both right and left limbs. We used DLC (Mathis et al. 2018) to track the iliac crest, hip, knee, ankle, hindpaw, shoulder, elbow, wrist, and forepaw coordinates, as well as the beam surface to define our vertical baseline. The number of slips and the phases of the step cycle (beginning of swing, end of swing, and end of stance) were manually annotated. Slips or pauses on the beam were excluded from the kinematic analysis. Please note that 24-month-old mice display an increased number of slips on the narrowest beam (5 mm), thus we analysed less animals compared to the other tasks.

Human participants

Participants meeting the following criteria were eligible for inclusion in the study: Age between 21 and 90 years, written informed consent, absence of neurological or psychiatric diseases and no health conditions affecting the locomotor system. The study was conducted according to the principles of the Declaration of Helsinki and approved by the local ethics committee of the Faculty of Medicine at University of Cologne (21-1418_1).

The final sample consisted of 24 individuals, including 13 younger participants (age [mean ± SD]: 27.0 ± 3.6 years, age range: 21 to 35 years; 10 females) and 11 older participants (age [mean ± SD]: 71.9 ± 5.1 years, age range: 65 to 85; 5 females). There were no significant differences between the two age groups with regard to sex ($\chi^2 = 1.354$, $p = 0.245$), body height ($t = 0.373$, $p = 0.713$) and weight ($t = -1.856$, $p = 0.077$; see **Table 1**).

Table 1.

Demographic data of the groups with younger and older healthy human participants.

Potential group differences in gender were assessed with a chi-square test, while group differences in age, height and weight were assessed using two-sample t-tests.

Category	**Reported**	**Participants (N = 24)**		**p-value**
		Younger (N = 13)	**Older (N = 11)**	
Sex	m/f	3/10	6/5	0.245
Age [years]	mean ± SD	27.0 ± 3.6	71.9 ± 5.1	0.001
Height [m]	mean ± SD	1.73 ± 0.1	1.71 ± 0.1	0.713
Weight [kg]	mean ± SD	67.4 ± 11.4	77.5 ± 15.3	0.077

Gait laboratory

The gait assessments were carried out on a walkway (460 cm in length x 60 cm in width) located in the gait laboratory of the Department of Neurology at the University Hospital of Cologne. As part of the video-based markerless Simi™-system, the Simi™ Motion software (version 10.2.0) was used for the video recordings. Eight high-speed cameras (mvBlueCougar XD, Matrix Vision GmbH; 100 frames/second), strategically positioned in a circular arrangement around the walkway, recorded the participants' gait from eight different angles.

Gait assessment

At the beginning of the recording, participants were asked to stand at a marked position on one end of the walkway. After a verbal signal by the experimenter, they started walking at a convenient, self-generated speed to the other end of the walkway. At the end, they were asked to stop, turn around and walk back to the start position. When they arrived at the start position, participants stopped and turned around again to start the next walk on the walkway. Up to three trials (walking forth and back on the walkway) were performed by each participant.

(Pre-)Processing of human gait data

For pre-processing of the human gait data, three investigators examined frame-by-frame the videos using at least two cameras: one installed perpendicular to the sidewalk and one placed in line with the walkway. The investigator manually annotated the gait cycle phases in the Simi™ Motion software, i.e., the start of the swing phase, the end of the swing phase/start of the stance phase, and the end of the stance phase. More specifically, the toe-off moment of the feet was marked as the end of the stance phase and simultaneously as the start of the swing phase. The moment of the heel-strike was marked as the end of the swing phase and simultaneously as the start of the stance phase. Further, the video recordings were processed in the Simi™ Shape

software (version 5.0.0). For this purpose, each point in the room was assigned a coordinate on the axes x, y and z in advance. Based on these coordinates, the software was used to track movements by detection of silhouettes to reconstruct the joint kinematics as 3D coordinates (Braunias, 2016). After exporting this data, *AutogaitA* was used to statistically analyse the annotations and associated joint kinematics.

Experimental fly model

Adult male wild-type Canton-S *Drosophila melanogaster* flies were collected after eclosion and reared on a standard yeast-based medium (Backhaus et al., 1984) at 25°C and 65% humidity in a 12h:12h day/night cycle. Experiments were performed with either two to three days old flies (young group) or 21 to 22 days old flies (old group).

Motor behaviour test

For motion capture, tethered flies walked on a spherical treadmill (Berendes et al., 2016) and movements of the right hind leg were recorded from the side using a high-speed camera (acA1300-200um, Basler AG, Ahrensburg, Germany) equipped with a 50 mm lens (LM50JC1MS, Kowa Optical Products Co. Ltd. Nagoya, Japan). Videos were recorded at 400 Hz and a resolution of 912 by 550 pixels. To convert pixels into metric scale, the camera was calibrated with a custom-made checkerboard pattern (7 x 6 squares with size 399 µm x 399 µm per square) developed on a photographic slide (Gerstenberg Atelier für Visuelle Medien, Templin, Germany). The conversion factor of 5.883 ± 0.198 µm per pixel (mean ± standard deviation) was determined by analysing the side length of 1850 squares from 74 images of the checkerboard.

2-D kinematic reconstructions

DLC (Mathis et al., 2018) was used for automated tracking of the leg landmarks in the videos. Six landmarks were tracked on the hind leg: the thorax-coxa (ThCx) joint, coxa-trochanter

(CxTr) joint, femur-tibia (FeTi) joint, tibia-tarsus (TiTar) joint and the tarsus tip (Tar). For this, a ResNet-50 network was trained with a training set containing 655 images. Resulting leg landmark predictions were inspected visually and corrected manually as needed with a custom-made graphical user interface software. Begin and end time points for swing and stance were identified manually for each step.

Supplementary Material

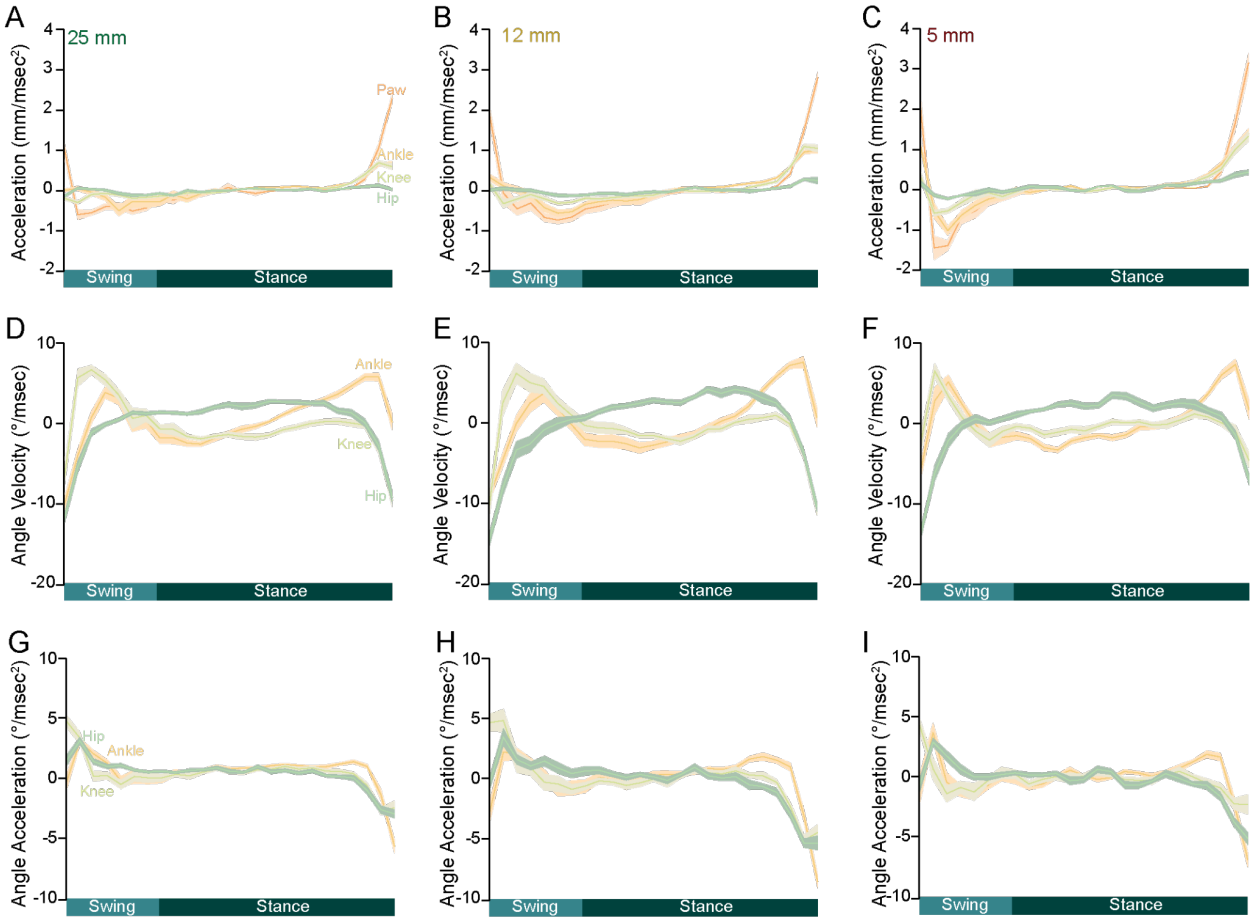

Figure S1. Beam width-induced changes in kinematics. A-G*) Acceleration of individual joints (****A-C****), angular velocities (****D-F****) and acceleration (****G-I****) during a normalised step cycle on the 25 mm (****A,D,G****), 12 mm (****B,E,H****) and 5 mm (****C,F,I****) beams. Data are presented as mean±SEM, with mean indicated by a darker line and SEM as shaded areas.*

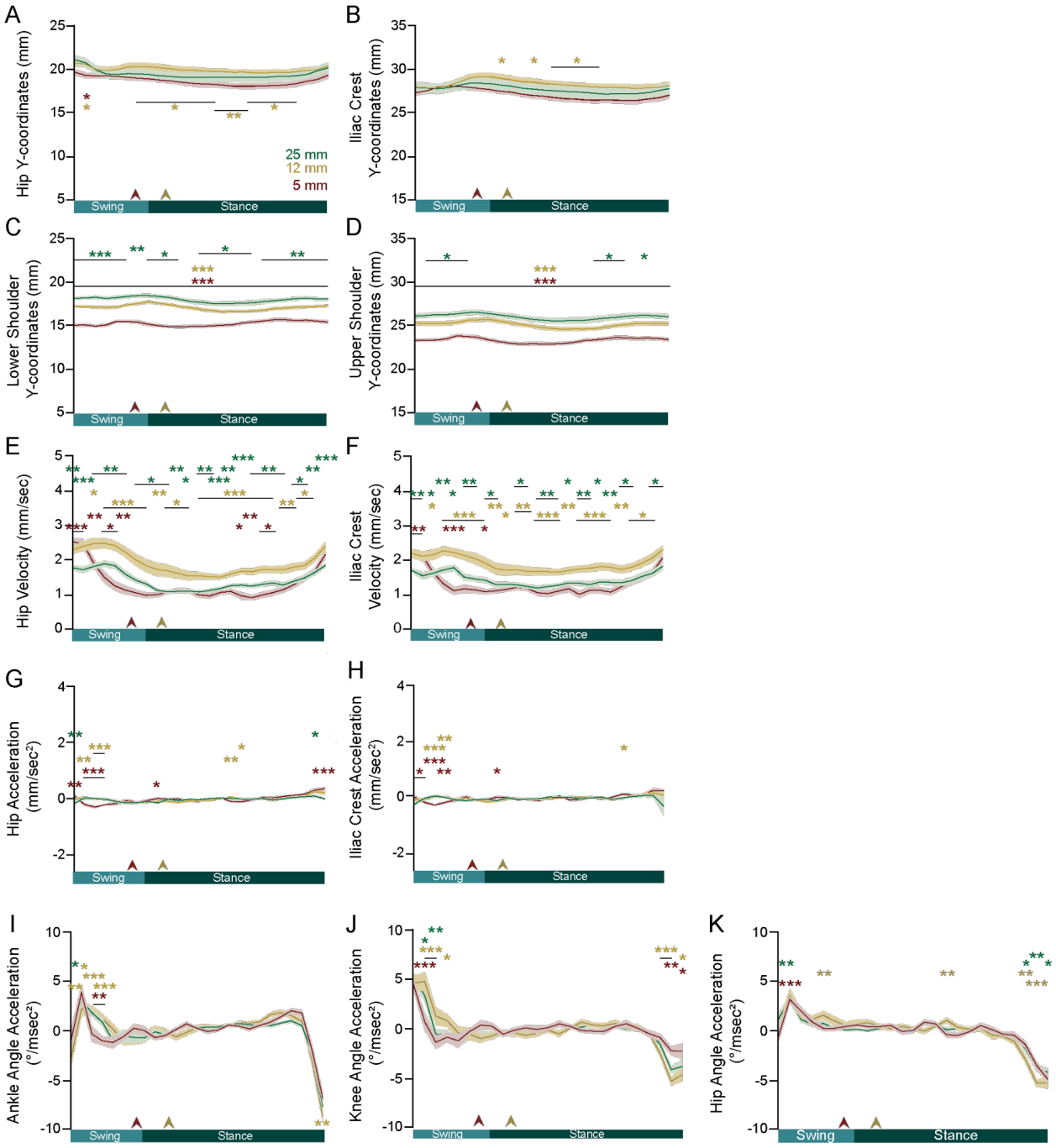

Figure S2. Kinematics of beam adaptation. *A-D) Changes in vertical position (y-coordinate) of hip (**A**), iliac crest (**B**), lower (**C**) and upper (**D**) shoulder as mice cross the 25 mm (green), 12 mm (yellow) and 5 mm (red) beams. **E,F**) Beam width-induced changes in hip (**E**) and iliac crest (**D**) joint velocity. **G,H**) Beam width-induced changes in hip (**G**) and iliac crest (**H**) acceleration **I-K**) Changes in ankle (**I**), knee (**J**) and hip (**K**) angular acceleration. Data are presented as mean±SEM, with mean indicated by a darker line and SEM as shaded areas. The yellow and red arrowheads indicate the swing duration when mice crossed the 25 and 15 mm beams, respectively. Statistical significance was calculated with a two-way ANOVA followed by Tukey's post-hoc test, 25 mm vs 5 mm (red asterisks), 12 mm vs 5 mm (yellow asterisks), 25 mm vs 12 mm (green asterisks).*

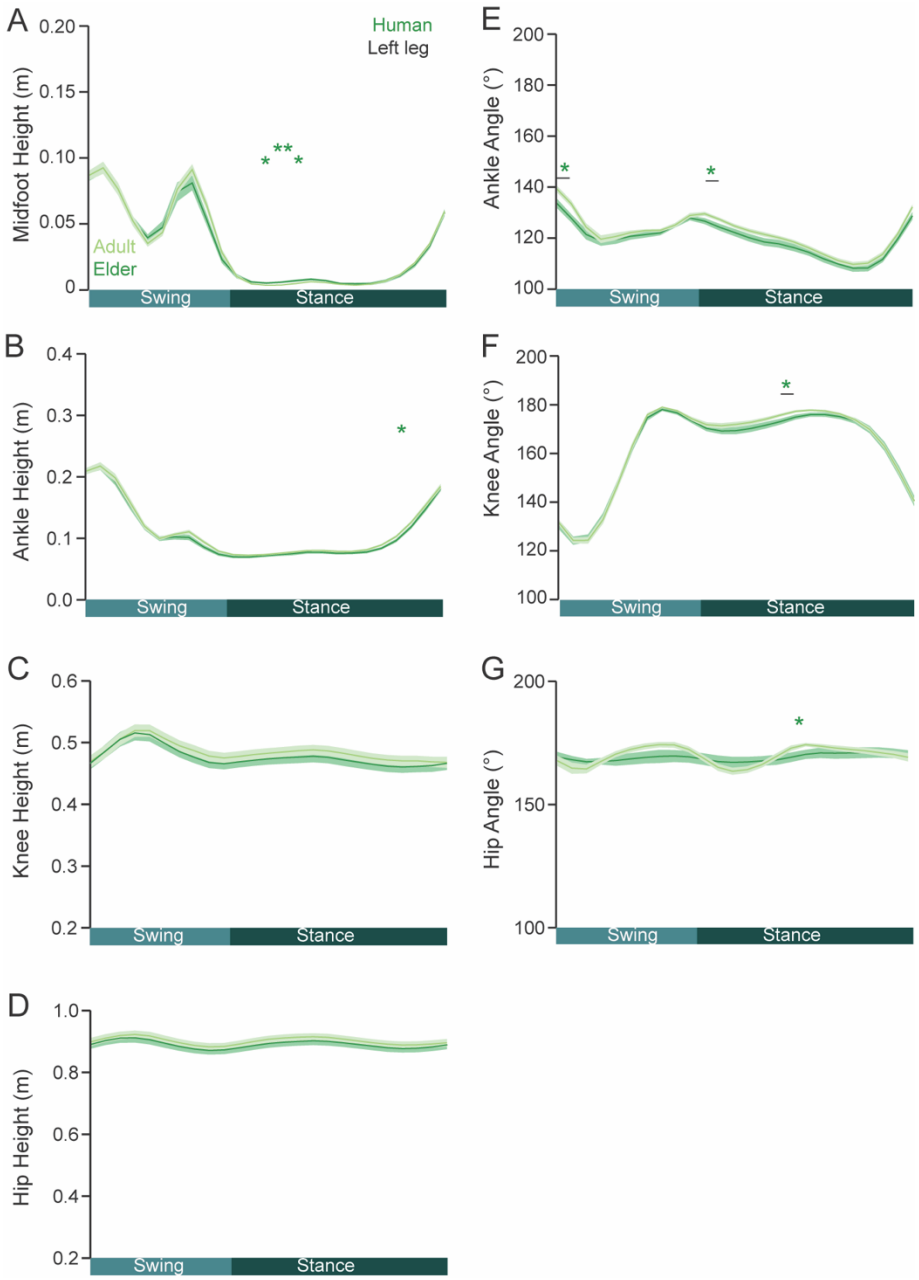

Figure S3. Age-dependent changes in human kinematics. *Changes or lack thereof in vertical position (y-coordinate) of the midfoot (**A**), ankle (**B**) knee (**C**) hip (**D**) joints and the ankle (**E**), knee (**F**) and hip (**G**) angles in the human left leg. Statistical significance was calculated with a two-way ANOVA followed by Tukey's post-hoc test*

References

Aljovic, A., Zhao, S., Chahin, M., de la Rosa, C., Van Steenbergen, V., Kerschensteiner, M., & Bareyre, F. M. (2022). A deep learning-based toolbox for Automated Limb Motion Analysis (ALMA) in murine models of neurological disorders. *Communications Biology*, *5*(1). https://doi.org/10.1038/s42003-022-03077-6

Arac, A., Zhao, P., Dobkin, B. H., Carmichael, S. T., & Golshani, P. (2019). DeepBehavior: A deep learning toolbox for automated analysis of animal and human behavior imaging data. *Frontiers in systems neuroscience*, *13*, 20.

Backhaus, B. S. E., Sulkowski, E. & Schlote, F. W. (1984). A semi-synthetic, general-purpose medium for Drosophila melanogaster. *Drosophila Information Service,* 60, 210–212.

Berendes, V., Zill, S. N., Büschges, A. & Bockemühl, T. (2016). Speed-dependent interplay between local pattern-generating activity and sensory signals during walking in Drosophila. *Journal of Experimental Biology,* 219, 3781–3793.

Boyer, K. A., Johnson, R. T., Banks, J. J., Jewell, C., & Hafer, J. F. (2017). Systematic review and meta-analysis of gait mechanics in young and older adults. Experimental gerontology, 95, 63-70.

Braunias, K. (2016). *Evaluation of markerless 3D joint position accuracy using high end vs. low end camera setups* on simi.com. Access date: 18.12.2023 http://www.simi.com/fileadmin/user_upload/Dokumente/Downloads/Markerless_3D_joint_position_accuracy_using_high_end_vs_low_end_camera_setups.pdf

Dougherty, K. J. (2023). *Distinguishing subtypes of spinal locomotor neurons to inform circuit function and dysfunction.* Current Opinion in Neurobiology, 82, 102763.

Dunn, T. W., Marshall, J. D., Severson, K. S., Aldarondo, D. E., Hildebrand, D. G., Chettih, S.

N., ... & Ölveczky, B. P. (2021). Geometric deep learning enables 3D kinematic profiling across species and environments. *Nature methods*, *18*(5), 564-573.

Gatto, G., Bourane, S., Ren, X., Di Costanzo, S., Fenton, P.K., Halder, P., Seal, R.P., Goulding, M.D. (2021) A Functional Topographic Map for Spinal Sensorimotor Reflexes. *Neuron.* 109(1):91-104.e5.

Gosztolai, A., Günel, S., Lobato-Ríos, V. *et al.* LiftPose3D, a deep learning-based approach for transforming two-dimensional to three-dimensional poses in laboratory animals. *Nat Methods* 18, 975–981 (2021). https://doi.org/10.1038/s41592-021-01226-z

Hosseini, M. (2024). AutoGaitA - Automated Gait Analysis in Python (0.0.4). Zenodo. https://doi.org/10.5281/zenodo.10947621

Inayat, S., Singh, S., Ghasroddashti, A., Qandeel, Egodage, P., Whishaw, I. Q., & Mohajerani, M. H. (2020). A Matlab-based toolbox for characterizing behavior of rodents engaged in string-pulling. *Elife*, *9*, e54540.

Karashchuk, P., Rupp, K. L., Dickinson, E. S., Walling-Bell, S., Sanders, E., Azim, E., ... & Tuthill, J. C. (2021). Anipose: A toolkit for robust markerless 3D pose estimation. *Cell reports*, *36*(13).

Luxem, K., Sun, J. J., Bradley, S. P., Krishnan, K., Yttri, E., Zimmermann, J., ... & Laubach, M. (2023). Open-source tools for behavioral video analysis: setup, methods, and best practices. *elife*, *12*, e79305.

Maris, E., & Oostenveld, R. (2007). Nonparametric statistical testing of EEG- and MEG-data. *Journal of neuroscience methods*, *164*(1), 177–190. https://doi.org/10.1016/j.jneumeth.2007.03.024

Mathis, A., Mamidanna, P., Cury, K. M., Abe, T., Murthy, V. N., Mathis, M. W., & Bethge, M. (2018). DeepLabCut: Markerless pose estimation of user-defined body parts with deep learning. *Nature Neuroscience*, *21*(9), Article 9. https://doi.org/10.1038/s41593-018-0209-y

Nilsson, S. R., Goodwin, N. L., Choong, J. J., Hwang, S., Wright, H. R., Norville, Z. C., ... & Golden, S. A. (2020). Simple Behavioral Analysis (SimBA)–an open source toolkit for computer classification of complex social behaviors in experimental animals. *BioRxiv*, 2020-04.

Pereira, T. D., Tabris, N., Matsliah, A., Turner, D. M., Li, J., Ravindranath, S., ... & Murthy, M. (2022). SLEAP: A deep learning system for multi-animal pose tracking. *Nature methods*, *19*(4), 486-495.

Stolze, H., Kuhtz-Buschbeck, J. P., Drücke, H., Jöhnk, K., Diercks, C., Palmié, S., Mehdorn, H. M., Illert, M., & Deuschl, G. (2000). Gait analysis in idiopathic normal pressure hydrocephalus--which parameters respond to the CSF tap test?. *Clinical neurophysiology : official journal of the International Federation of Clinical Neurophysiology*, *111*(9), 1678–1686. https://doi.org/10.1016/s1388-2457(00)00362-x

Tutas, J., Tolve, M., Oezer Yildiz, E., Ickert, L., Klein, I., Hosseini, M., ... & Kononenko, N. L. (2024). Autophagy regulator ATG5 preserves cerebellar function by safeguarding its glycolytic activity. *bioRxiv*, 2024-01.

Weinreb, C., Pearl, J., Lin, S., Osman, M. A. M., Zhang, L., Annapragada, S., ... & Datta, S. R. (2023). Keypoint-MoSeq: parsing behavior by linking point tracking to pose dynamics. *BioRxiv*.

Winiarski, S. (2003). Human locomotion analysis technique with SIMI Motion. *Acta of Bioengineering and Biomechanics*, *5*(1), 544-50.

Zanardi, A. P. J., da Silva, E. S., Costa, R. R., Passos-Monteiro, E., Dos Santos, I. O., Kruel, L. F. M., & Peyré-Tartaruga, L. A. (2021). Gait parameters of Parkinson's disease compared with healthy controls: A systematic review and meta-analysis. *Scientific reports*, *11*(1), 752.